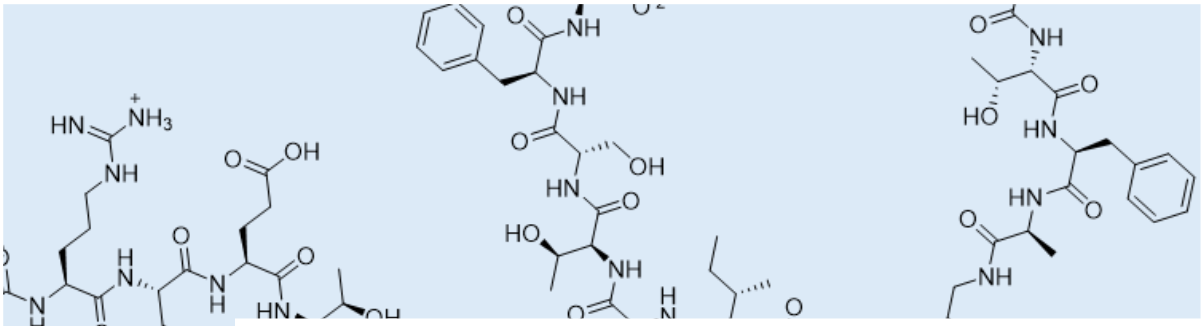

Structure Affinity Relationship Study of Macrocyclic Peptide Scaffold Binding to PSD-95

Frida Berg

CENTRUM FOR ANALYSIS AND SYNTHESIS | DEPARTMENT OF CHEMISTRY | FACULTY OF ENGINEERING LTH | LUND UNIVERSITY

In collaboration with:

DEPARTMENT OF DRUG DESIGN AND PHARMACOLOGY | UNIVERSITY OF COPENHAGEN

2024

MASTER THESIS

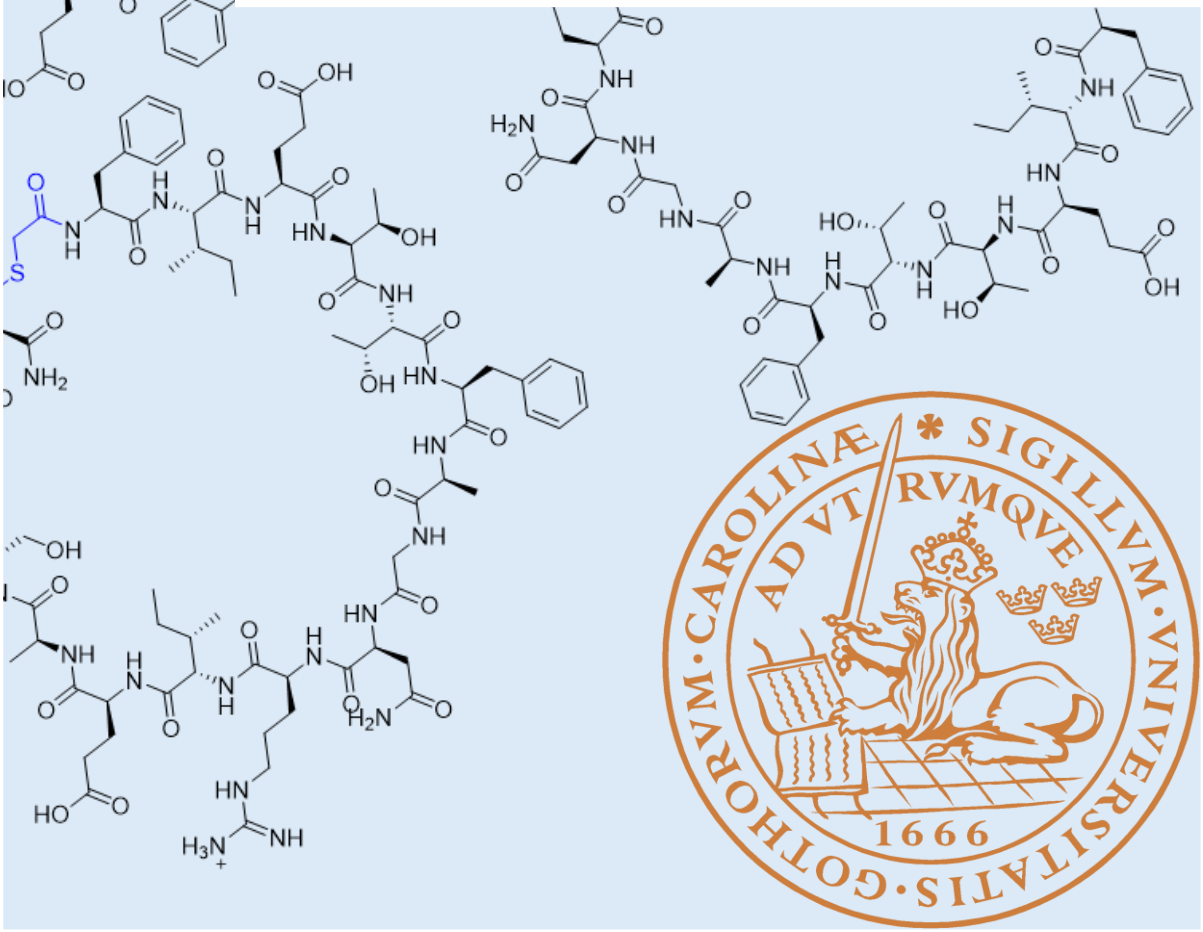

Structure Affinity Relationship Study of Macrocyclic Peptide Scaffold Binding to PSD-95

Subject: KASM05 Degree Project in Organic Chemistry for Engineers

Author: Frida Berg

Supervisor at University of Copenhagen: Kristian Strømgaard, Professor, Department of Drug Design and Pharmacology, University of Copenhagen

Supervisor at LTH: Ulf Ellervik, Professor, Center for Analysis and Synthesis, Department of Chemistry, Faculty of Science, Lund University

Examiner: Ulf Nilsson, Professor, Professor, Center for Analysis and Synthesis, Department of Chemistry, Faculty of Science, Lund University

Acknowledgements

This thesis details the research conducted during my MSc project in organic chemistry, as part of my master's in biotechnology engineering. All experiments were carried out from January to June 2024 in the Strømgaard lab at the Center for Biopharmaceuticals, Department of Drug Design and Pharmacology, Faculty of Health and Medical Sciences, University of Copenhagen. This project was performed under the supervision of Professor Kristian Strømgaard and Assistant Professor Christian Reinhard O. Bech-Bartling.

Firstly, I would like to express my deepest gratitude to Professor Kristian Strømgaard for allowing me to join his esteemed research group. During my time in the Strømgaard group, I gained valuable insights into cutting-edge research in peptides and proteins. This experience has equipped me with essential knowledge and skills for my future.

I am also immensely grateful to my advisor, Christian Reinhard O. Bech-Bartling, for his invaluable guidance, encouragement, and expertise. Your support throughout the lab work and assistance with writing this thesis have been irreplaceable.

Special thanks to all members of the Strømgaard group for making my time in Copenhagen enjoyable and for their warm and welcoming nature. It has been a pleasure to work with you, and I appreciate the support and encouragement you provided along the way.

Lastly, on a personal note, I would like to thank my family and friends for their support and encouragement throughout this journey.

Cyclic Peptides: A Novel Approach to Stroke Protection

Acute ischemic stroke is a leading cause of death and disability worldwide. Despite advances in medical science, effective treatments to reduce stroke-induced damage remain limited. However, new research into neuroprotective strategies is showing promise. One such strategy targets a protein inside postsynaptic nerve cells called postsynaptic density protein 95 (PSD-95), which is crucial in regulating brain cell survival after a stroke.

During an ischemic stroke, blood vessels to the brain are blocked, preventing oxygen from reaching brain tissue. This blockage leads to the formation of toxic compounds that harm the brain and cause neuronal cell death. By blocking PSD-95 protein, we hope to prevent neuronal cell death and enhance brain recovery following a stroke. This master thesis research focuses on developing cyclic peptides that inhibit a specific part of the PSD-95 protein to stop the formation of these toxic compounds during a stroke. To achieve this, the project was based on a lead peptide known to bind to PSD-95 with high affinity. An "alanine scan" was conducted to understand how each part of this peptide interacts with PDZ2, a domain of PSD-95. This involved creating variants of the peptide where specific amino acids were replaced with alanine, thereby losing the unique properties of those side chains. These variants were tested to assess their binding affinity to the PSD-95 protein. Additionally, the stability of the original peptide was assessed to ensure it could withstand enzymatic breakdown in the body.

The study found that certain amino acids within the peptide are crucial for binding to PSD-95. Specifically, three amino acids were essential for binding, while two more played significant roles. In contrast, three amino acids were less important for binding. Moreover, stability tests demonstrated that the original peptide is stable against the tested enzyme, indicating it is likely to remain intact and effective in the body. These findings represent a significant step towards developing a new treatment for stroke. By understanding which parts of the peptide are most important for binding to PSD-95, the peptide designs can be refined and improved. Future work will focus on completing the alanine scan and exploring additional modifications to further enhance the peptide’s effectiveness and cell permeability.

In conclusion, targeting PSD-95 with specially designed cyclic peptides offers a promising new approach to reducing stroke damage and promoting brain recovery. This master thesis research provides valuable insights into how these peptides interact with PSD-95 and lays the groundwork for developing more effective neuroprotective therapies.

Abstract

Acute ischemic stroke is one of the major causes of death and disability worldwide. New neuroprotective strategies have emerged, with the postsynaptic density protein 95 (PSD-95) identified as a promising target. PSD-95 plays a crucial role in controlling downstream NMDA receptors and neuronal death. Consequently, therapies targeting PSD-95 could mitigate stroke damage while promoting brain protection and recovery.

This project focused on investigating cyclic peptides for the inhibition of the PDZ2 domain of PSD-95. The study was based on a lead peptide binding to the PDZ2 domain with a K_i value of 0.3 μM. To further understand its interaction with PDZ2, an alanine scan was conducted, synthesizing alanine variants of the parent 17-mer cyclic peptide. These peptides were evaluated for their binding to PDZ2 using a fluorescence polarization assay to assess the contribution of each residue. Additionally, the plasmin stability of the parent 17-mer peptide was investigated.

Due to synthesis challenges, a complete alanine scan was not possible; only nine out of the planned 14 peptides were synthesized and tested for PDZ2 binding. Results indicated that residues E3, E12, and T13 are crucial for binding to PDZ2, while I11 and F15 are also highly important. In contrast, I2, T5, S14, and T16 were found to be less significant for binding. Stability assays demonstrated that the parent 17-mer peptide appears to be metabolically stable when tested in a plasmin stability assay.

Future work should aim to complete the alanine scan and include additional positional scans, such as N-methylated amino acid and D-amino acid scans, to further evaluate each residue's function. Moreover, efforts should be made to miniaturize the 17-mer lead peptide by removing less important residues, potentially enhancing cell permeability—a highly desirable characteristic when targeting PSD-95.

List of Abbreviations

AA - L-α-Amino acid
AMPAR - α-Amino-3-hydroxy-5-methyl-4-isoxazoleproprionic acid receptor
ATP - Adenosine triphosphate
BBB – Blood brain barier
BSA - Bovine serum albumin
CAA - Chloroacetic acid
Da - Dalton
DCM - Dichloromethane
DIPEA - N,N-Diisopropylethylamine
DIC - N,N'-Diisopropylcarbodiimide
DNA - Deoxyribonucleic acid
DMSO - Dimethyl sulfoxide
Fmoc - 9-fluorenylmethoxycarbonyl
GK - Guanylate kinase
Gua - N-terminal tetramethylguanidinium termination
HATU - 1-[Bis(dimethylamino)methylene]-1H-1,2,3-triazolo[4,5-b]pyridinium 3-oxid hexafluorophosphate
HBTU - 2-(1H-Benzotriazole-1-yl)-1,1,3,3-tetramethyluronium hexafluorophosphate
HCTU- O-(1H-6-Chlorobenzotriazole-1-yl)-1,1,3,3-tetramethyluronium hexafluorophosphate
HPLC - High-performance liquid chromatography
KCN – Potassium cyanide
FP - Fluorescence polarization
K_d - Dissociation constant
K_i - Inhibition constant
LC-MS - Liquid chromatography-mass spectrometry
MAGUK - Membrane-associated guanylate kinase
Mmt - 4-Methoxytrityl
NMDAR - N-Methyl-D-aspartate receptor
NMR - Nuclear magnetic resonance
nNOS - Neuronal nitric oxide synthase
NO - Nitric oxide
NPEG - Amino-polyethylene glycol
Oxyma - 2-cyano-2-(hydroxyimino)acetate
PBS - Phosphate-buffered saline
PDZ - PSD-95/Dlg/ZO-1
PDB - Protein Data Bank
PEG - Polyethylene glycol
Pip - Piperidine adduct
PSD-95 - Postsynaptic density protein 95

PPI - Protein-protein interaction
PyBOP - Benzotriazol-1-yloxytripyrrolidinophosphonium hexafluorophosphate
RaPID - Random nonstandard Peptides Integrated Discovery
SH3 - Src homology 3
SPPS - Solid-phase peptide synthesis
TFA - Trifluoroacetic acid
TC - Test cleavage
tPA - Tissue plasminogen activator
Thp - Tetrahydropyranyl
UPLC - Ultra-performance liquid chromatography

AAs are referred to as their three-letter code/single letter in the text. Peptide sequences are written with capital letters.

Crystal structures were made into figures by exporting the PDB files in PyMOL by Schrödinger.

Figures were made either with Biorender.com or with ChemDraw 23.1.1.

Table of Contents

1 Introduction

1.1 Cerebral Ischemia

The human brain accounts for 25% of the metabolic demand in a person and requires complex mechanisms to maintain blood flow, requiring about 50 ml of blood per 100g of brain tissue per minute. When the blood flow is compromised it results in the most common mechanism of brain dysfunction and damage, namely cerebral ischemia. The term 'stroke' is broad and includes all neurological injuries inflicted by vascular causes. However, ischemic stroke makes up 87% of all strokes, making it the most common type. Ischemic stroke is also a major cause for both death and disability in the world. (DeSai and Hays Shapshak, 2023)

Obstruction of arterial blood flow to the brain often results in focal brain ischemia, meaning it affects a certain area of the brain. If the ischemia persists long enough it results in irreversible neural loss. After as little as five minutes, a lack of oxygen and glucose to ischemic brain tissue results in necrosis. (DeSai and Hays Shapshak, 2023) During cerebral ischemia there are two distinguishable areas that are affected, the infarct core and the penumbra. The infarct core will be irreversibly damaged; however, the penumbra can still be recovered with neuroprotective strategies. The penumbra does not suffer complete loss of blood flow and is still metabolically active. It is only functionally impaired and can be saved if the blood flow is restored or the cells become more resistant. The infarct core can also expand due to secondary damage of the penumbra and suffer neuronal death due to excitotoxicity. (Ugalde-Triviño and Díaz-Guerra, 2021) Excitotoxicity occurs when cells are exposed to high concentrations of excitatory neurotransmitters which can mediate cell death of central neurons. Excitotoxicity often is cell specific and is in most cases caused by glutamate. (Choi, 1992)

1.2 Postsynaptic Density Protein-95 (PSD-95)

When excitatory synaptic transmission occurs, glutamate is released into the synaptic cleft. Glutamate diffuses across the cleft and binds to postsynaptic N-methyl-D-aspartate receptors (NMDARs) and α-amino-3-hydroxy-5-methyl-4-isoxazolepropionic acid receptors (AMPARs). NMDARs are glutamate-gated cation channels characterized by calcium permeability and play an important role during cerebral ischemia (Blanke and VanDongen, 2009). They are also central to survival, neuronal transmission, synaptic plasticity, and memory. NMDARs are heterotetramers consisting of two GluN1 subunits, one GluN2 subunit, and one GluN3 subunit (Ugalde-Triviño and Díaz-Guerra, 2021).

Right beneath the membrane of postsynaptic neurons is the postsynaptic density protein-95 (PSD-95), which interacts with NMDARs (Serrano et al., 2022) (Ugalde-Triviño and Díaz-Guerra, 2021). PSD-95 is composed of multiple protein-protein interacting domains connected via flexible linkers and is part of the membrane-associated guanylate kinases (MAGUKs) superfamily. The

sequence of the domains from the N terminus comprises three PSD-95/Discs Large/ZO-1 (PDZ) domains, one Src homology 3 (SH3) domain, and one nonenzymatic guanylate kinase (GK) domain (see Figure 1.1) (Zhang et al., 2013). PSD-95 is organized into two supramodules, resulting in a super tertiary structure. The first supramodule, called the PDZ1-2 supramodule, contains PDZ1 and PDZ2, which are class I PDZ domains. PDZ1-2 forms a ternary complex with the NMDAR-GluN2B subunits and neuronal nitric oxide synthase (nNOS). The PDZ domains interact with the C-terminus of GluN2B. PDZ3, SH3, and GK form the second supramodule, known as the P-S-G supramodule (Ugalde-Triviño and Díaz-Guerra, 2021).

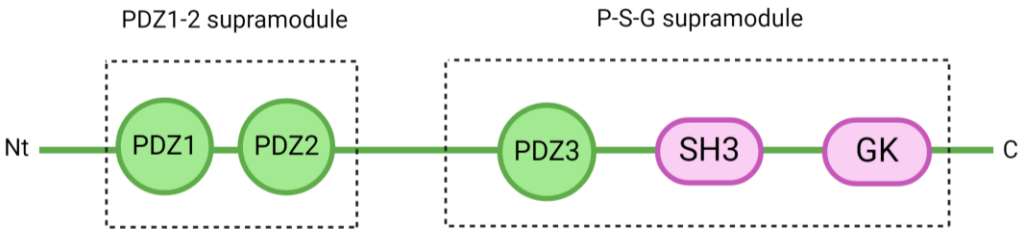

Figure 1.1: Schematic representation of the domain arrangement in PSD-95. PSD-95/Discs Large/ZO-1 (PDZ); Src homology 3 (SH3); nonenzymatic guanylate kinase domain (GK). (Zhang et al., 2013)

When a stroke occurs, there is a loss of oxygen and glucose resulting in a decrease of ATP formation. The decrease in ATP concentration is followed by membrane depolarization and release of excitatory neurotransmitters such as glutamate into the synaptic cleft. This causes NMDAR overactivation, a large influx of Ca^{2+} into the postsynaptic density and ultimately excitotoxicity. (Balboa et al., 2022) Nitric oxide (NO) can form oxidant peroxynitrite by reacting with cell superoxide free radicals. Oxidant peroxynitrite is highly reactive and can cause oxidation of proteins and lipids as well as DNA damage. This can in turn lead to activation of apoptotic factors and trigger cell death. The process is depicted in *Figure 1.3.* (Ugalde-Triviño and Díaz-Guerra, 2021)

PSD-95 has become a promising target for therapeutic strategies due to the role it plays in controlling downstream NMADRs and neuronal death. Such potential therapies could help reduce stroke damage while protecting and recovering the ischemic penumbra. They could also be used to treat other various neurodegenerative diseases that are also associated with excitotoxicity. (Ugalde-Triviño and Díaz-Guerra, 2021)

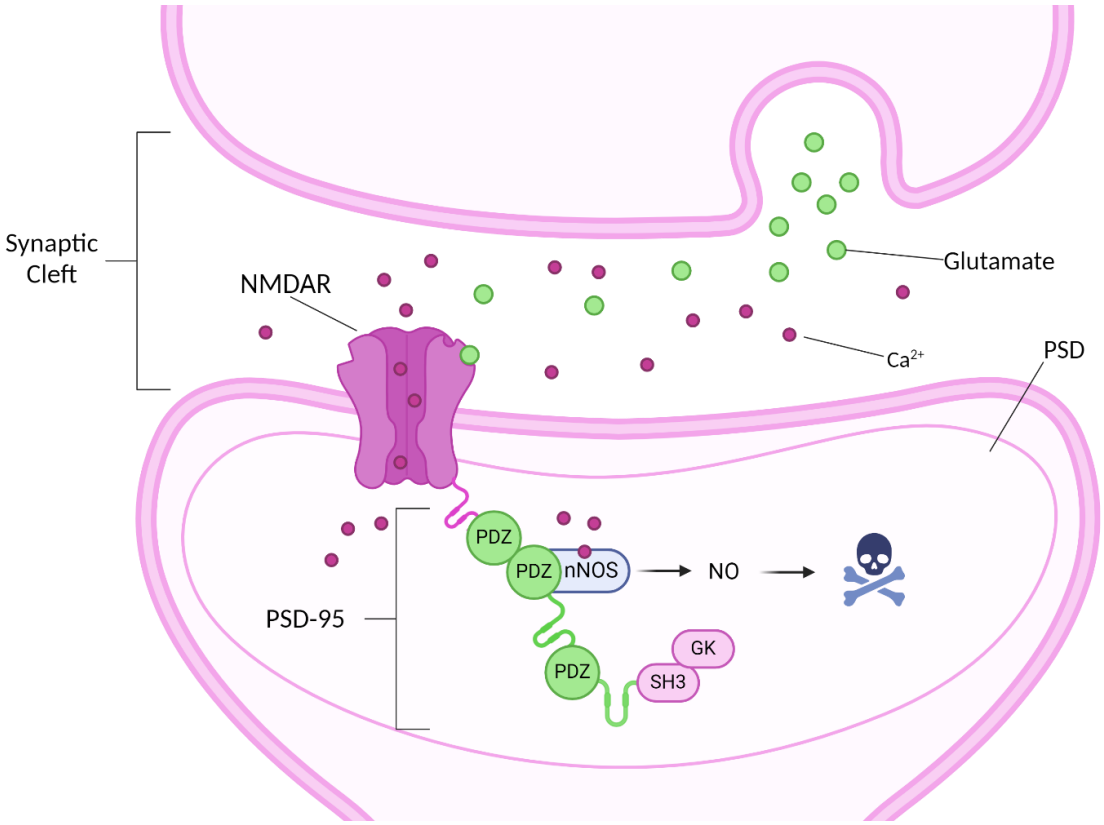

Figure 1.3: Schematic representation of the synaptic cleft and the role PSD during stroke. Excessive release of glutamate into the synaptic cleft leading to overactivation of NMDARs and high Ca^{2+} influx into the PSD. Ca^{2+} activates nNOS, leading to NO formation, excitotoxicity and ultimately cell death. (Balboa et al., 2022)

The PDZ domains consists of 80-100 AAs organized in six β-sheets and two α-helices. Through NMR and X-ray crystallography along with computational methods insight has been provided in the structure of the PDZ protein-protein interactions (PPIs) (see *Figure 1.2 A*). Class I PDZ domains canonically bind to the C-terminus of target proteins where the C-terminal carboxylate forms hydrogen-bonds to the loop between βB and αB of the PDZ2. This is how they interact with the GluN2B subunit of NMADRs. The side chain of the C-terminal residue is also inserted into a hydrophobic pocket of the βB in canonical binding mode (see *Figure 1.2 B*). Furthermore, ligands can bind to the PDZ domain through internal motifs which also rely on the insertion of a hydrophobic residue in the binding pocket of βB. However, this binding also includes another hydrophobic residue or hydrogen bond interaction at position -2. The ligand can also interact at position +1 or +2 through negatively charged residues acting as a substitute for the carboxylic acid C-terminal. (Christensen et al., 2019) The PDZ domain can also bind to internal β-hairpin structure of interacting proteins. The PSD-95 PDZ2 domain binds to the nNOS protein in this way where position 0 is a phenylalanine buried in the hydrophobic pocket. The β-loop resembles the binding through internal motifs and covers a larger surface area which stabilises the inserted β-sheet (see *Figure 1.2 C*). (Christensen et al., 2019) (Lee and Zheng, 2010)

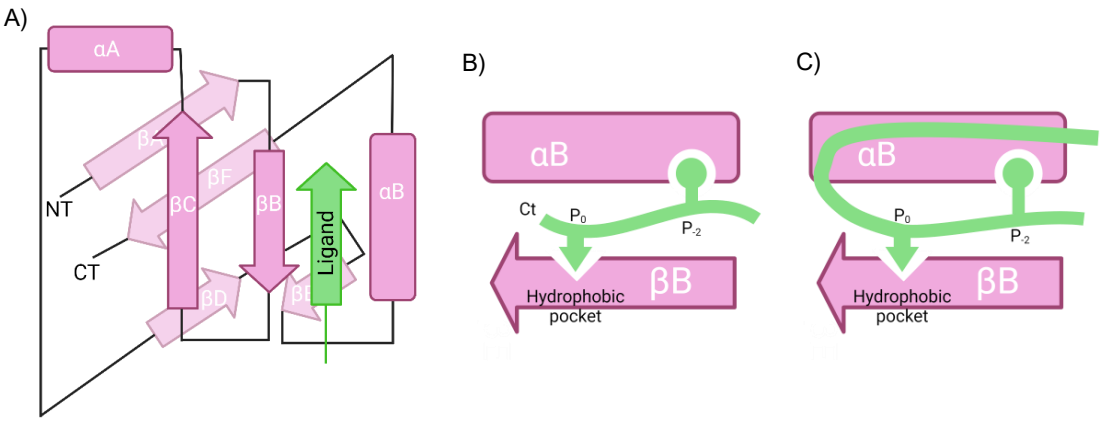

Figure 1.2: Schematic structure and binding modes of the PDZ2 domain of PSD-95. A) Schematic structure of the PDZ2 domain displaying α-helices, β-turns and the ligand (green) binding pose. B) Canonical binding of carboxylic C-terminal to PDZ2. C) Non-canonical binding of β-hairpin structures to PDZ2. (Christensen et al., 2019)

1.3 Neuroprotective strategies

By inhibiting the PDZ1-2 domains of PSD-95 the formation of the ternary complex nNOS/PSD-95/NMDAR can be inhibited. This will uncouple the harmful production of nitric oxide in the event of stroke and prevent excitotoxicity. Inhibition of PSD-95 does not affect the ion-influx through the NMDARs and therefore still allows for pro-survival signalling pathways mediated by the NMDAR. The 20-mer peptide Nerinetide (also known as Tat-NR2B9c or NA-1), developed by NoNO Inc. (Toronto, Canada), is a first-in-class compound targeting PSD-95 in the context of arterial ischemic stroke. (Aarts, 2002) (Bach et al., 2012) Nerinetide is composed of nine amino acids corresponding to the C-terminal of the GluN2B subunit of the NMDA receptor connected to the HIV-1 Tat peptide [YGRKKRRQRRR-KLSSIESDV]. (Aarts, 2002) Besides Nerinetide's insufficient stability profile, the peptide suffers from a relatively low affinity towards PSD-95. (Hill et al., 2020) In order to improve the affinity, the Strømgaard group designed the dimeric compound TAT-*N*-dimer, also known as AVLX-144 [YGRKKRRQRRR-*N*PEG^4-(IETDV)$_2$] which shows a 1000-fold improvement in affinity of (FP: K_i value = 4.6 nM). This compound has been shown to bind bivalently to the PDZ1-2 domains inhibiting PSD-95. AVLX-144 also displays extensive protease-resistance. (Bach et al., 2012)

1.3 Cyclic Peptides

Cyclic peptides are polypeptides of various lengths that are connected at distant positions to form a macrocyclic structure. (Ji, Nielsen and Heinis, 2024) The ring-formation can be done through various linkages of the peptides. In the so-called head-to-tail cyclization the N- and C-terminal of the peptide form an amide bond. Furthermore, there are other stable linkages such as ether, thioether, disulfide and ester bonds, which can be used to cyclize peptides. (Joo, 2012) The cyclic peptides found in nature show a range of biological activities such as signalling agents and chemical weapons for defence. Not only their function, but also their shape, size and composition

display large variation. Cyclic peptides also possess important properties such as high binding affinity and specificity, proteolytic stability, and sometimes improved membrane permeation. This makes macrocyclic peptides especially suitable as leads for drug development. Today there are already over 40 therapeutic cyclic peptides in use which are derived from natural cyclic peptides.
The increased binding affinity and specificity of cyclic peptides compared to linear peptides can be seen through e.g phage display. When screening peptides with phage display library cyclic peptides often perform better than linear peptides. The higher affinity can be explained by entropic effects. Cyclic peptides are less flexible than their linear counterparts, making the entropy cost lower when binding. (Ji, Nielsen and Heinis, 2024) The rigidity decreases the Gibbs free energy, which enhances binding and selectivity for the target. (Joo, 2012) Cyclic peptides also adopt a lot fewer conformations compared to linear peptides, rendering binding more likely to occur since the peptides are more probable to adopt the conformation required for binding due to fewer options.
There are two main reasons for the increased stability of cyclic peptides compared to linear. As mentioned before, they are not as flexible as linear peptides and therefore do not bind as easily to proteases. Since they do not adapt to the active site on these degradation enzymes, they are somewhat more metabolically stable. Some peptides are also cyclized via their terminal amino acids which prevents them from being broken down by exopeptidases.
The cyclic structure does not automatically increase membrane permeability of the peptides; however, it can be used to increase it. Cyclic peptides more easily form intramolecular H-bonds which reduces solvation. The cyclic structure can also hide some of the polar parts of a peptide inside the ring. Both properties increase the chances of membrane permeability which is highly useful when targeting intracellular proteins like PSD-95. (Ji, Nielsen and Heinis, 2024) To inhibit PSD-95 the peptide would have to cross both the blood brain barrier (BBB) and cell membrane.

2 Objectives

The Strømgaard group continuously works with cyclic peptides. In 2022, Flora Alexopoulou (PostDoc, Department of Drug Design and Pharmacology, University of Copenhagen, Copenhagen, Denmark) used the random nonstandard peptides integrated discovery platform, also called RaPID, to discover a cyclic 17-mer lead peptide (JFL-03) which binds to the PDZ2 domain of the PSD-95 with a K_i value of 0.3 μM. (Alexopoulou, 2022) In this project, JFL-03 has been further investigated to better understand its interaction with PDZ2 of PSD-95.

The specific objectives are:

- Synthesis of Ala-variants of the parent 17-mer cyclic peptide JFL-03 (Ala-scan).
- Optimization of synthesis and cyclization procedure.
- Evaluation of the binding of JFL-03 Ala variants to PDZ2 of PSD-95.

3 Methods

3.1 Solid Phase Peptide Synthesis (SPPS)

Solid phase peptide synthesis (SPPS) is a very practical form of peptide synthesis. The term peptide and stepwise synthesis from amino acids has been described for over a century. It is all based on a repetitive cycle of peptide elongation via a coupling reaction of amino acids and removing protecting groups. During SPPS the peptide chain is linked to an insoluble polymeric support, in this case resin, and the peptide is synthesized from C to N terminus using N^{α}-protected and side-chain protected amino acids. (Fields, 2001) The process of SPPS can be seen in *Figure 3.1* below and occurs in a stepwise cyclic manner. The resin is functionalized with a linker and placed in a reaction vessel with a filter at the bottom. The resin bound amino acid is N^{α}-deprotected and the next amino acid is added along with a coupling reagent to form the new peptide bond. The repeated washing in between the coupling steps allows for removal of side-products. The linker and side-chain protecting groups need to be stable during the reaction step as well as for the N^{α}-deprotection. When final cleavage is performed, the peptide is removed from the resin along with the side-chain protecting groups.

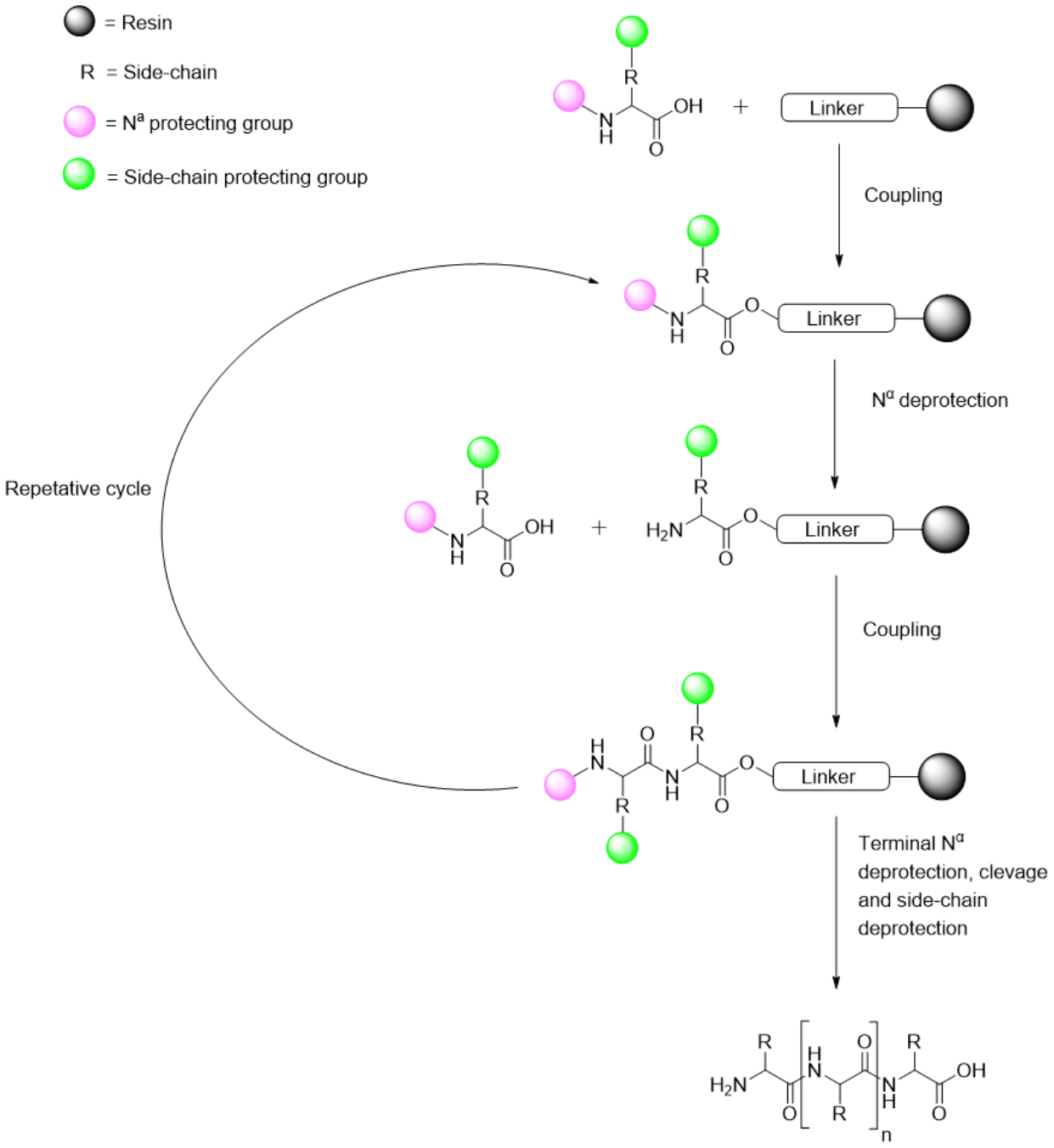

Figure 3.1: Schematic representation of SPPS. The peptide chain is linked to resin (grey) and the peptide is synthesized from C to N terminus using Nα-protected (pink) and side chain (green) protected amino acids. The repetitive cycle consists of peptide elongation via a coupling reaction of amino acids and removing protecting groups. During final cleavage the peptide is removed from the resin along with the side chain protecting groups.

3.1.1 Coupling Reagents

Coupling entails the amino group of one residue attacking the carbonyl carbon atom of the carboxyl-containing component, which has been activated through the introduction of an electron-withdrawing group (see *Figure 3.4*). The carboxyl is activated as an ester, usually with the use of diisopropylethylamine (DIPEA) for deprotonation. There are many different types of coupling reagents, the most traditional ones being carbodiimides like N,N'-Diisopropylcarbodiimide (DIC) (see *Figure 3.2*). The carbodiimide reacts with the carboxylic acid group of the amino acid or peptide to form an activated intermediate; O-acylisourea. The activated carboxylic acid intermediate then reacts with the amino group of another amino acid or peptide, forming an amide bond. The amino group acts as a nucleophile, attacking the carbonyl carbon of the activated carboxylic acid resulting in the formation of a new amide bond. This process releases a molecule of urea as a byproduct. (El-Faham and Albericio, 2011) Carbodiimides have high reactivity which is both an advantage and a disadvantage. The highly reactive intermediate O-acylisourea can cause side reactions which form N-acylurea, which is completely unreactive. Carbodiimides can also cause racemization. (Marder, Youval Shvo and Albericio, 2003) Due to this another nucleophilic additive such as ethyl 2-cyano-2-(hydroxyimino)acetate (Oxyma) is often used in combination with carbodiimides. They lower racemization and suppress N-acylurea formation. (SubirÃ3s-Funosas et al., 2009)

Other common coupling reagents are stand-alone immonium compounds such as O-(1H-6-Chlorobenzotriazole-1-yl)-1,1,3,3-tetramethyluronium hexafluorophosphate (HCTU) and phosphonium salts such as benzotriazol-1-yloxytripyrrolidinophosphonium hexafluorophosphate (PyBOP) (see *Figure 3.2*). The activation mechanism is the same, however with an in situ nucleophile (see *Figure 3.3*). (Marder, Youval Shvo and Albericio, 2003) (SubirÃ3s-Funosas et al., 2009)

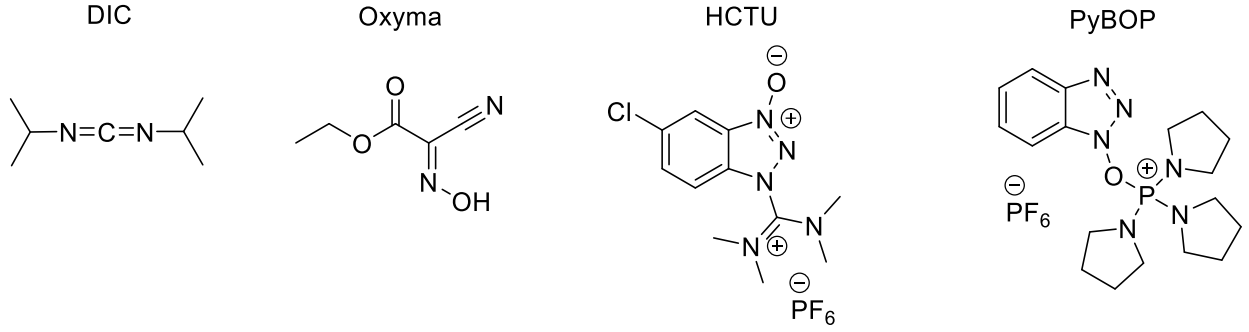

Figure 3.2: Structure of coupling reagents. Structure of coupling reagents from left to right; DIC, oxyma, HCTU and PyBOP.

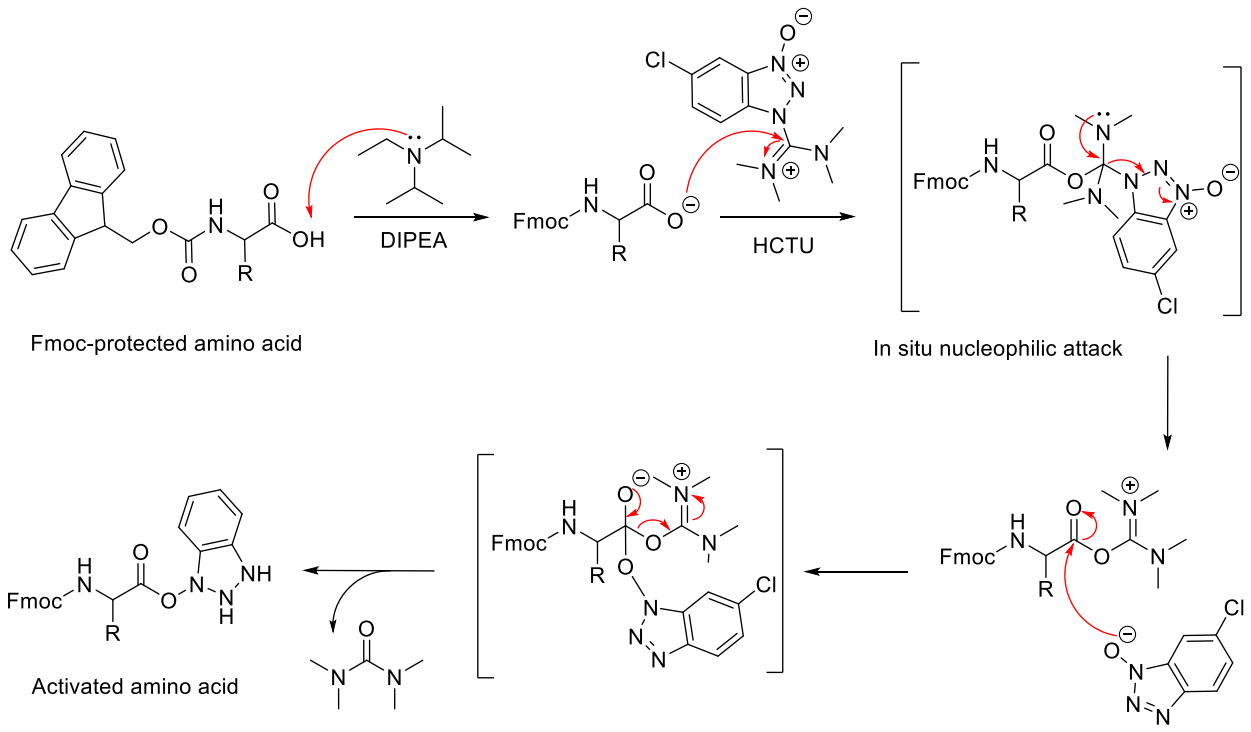

Figure 3.3: Activation of AA using HCTU and DIPEA. Activation mechanism of Fmoc-protected AA with coupling reagent HCTU and DIPEA.

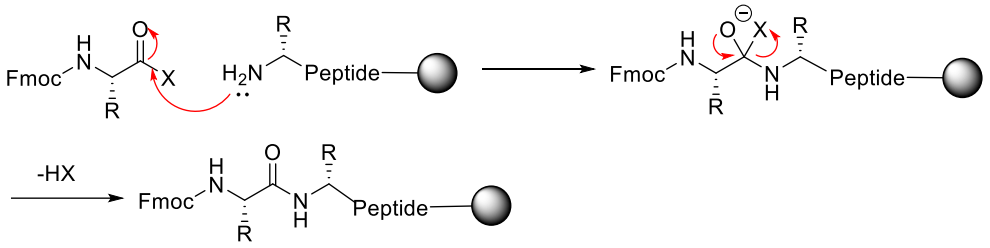

Figure 3.4: Coupling mechanism of AA. Coupling mechanism of AA (R=side chain, X= electron withdrawing group) to a peptide chain linked to resin (grey).

3.1.2 Fmoc protection

The most common N^{α}-protecting group used for SPPS is the 9-fluorenylmethoxycarbonyl (Fmoc). The advantages of using Fmoc as a protecting group are many. Fmoc building blocks are available at a low cost, there are many commercially available modified derivatives of Fmoc building blocks, and they avoid the usage of strong acids such as hydrogen fluoride. The use of Fmoc groups also provides an orthogonal combination of temporary and permanent protecting groups since they are labile under different conditions. (Behrendt, White and Offer, 2016) (Chan and White, 1999) The Fmoc protecting group is base-labile while the side-chain protecting groups and resin linkage is acid labile. The Fmoc group is removed with 20% piperidine in dimethylformamide (DMF) (see *Figure 3.*5) and side-chain protecting groups and resin linkage is removed with trifluoroacetic acid (TFA). (Chan and White, 1999)

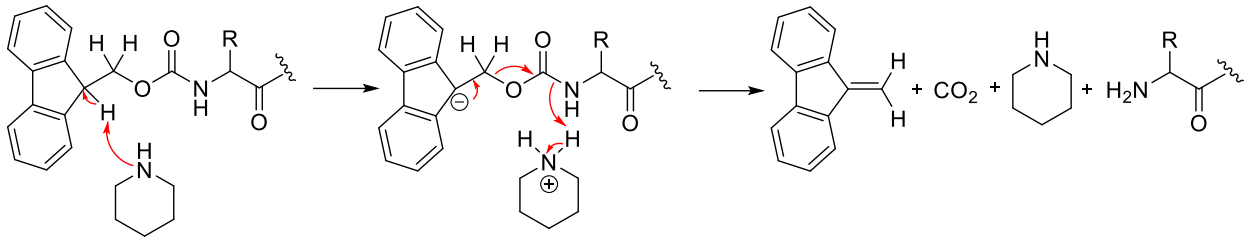

Figure 3.5: Fmoc deprotection of AA. Mechanism of Fmoc protection group removal of AA (R=side chain) using piperidine.

3.1.3 Pseudo Prolines

Pseudo-prolines can be used to minimize peptide aggregation for SPPS and thus improve solubility and coupling kinetics of the peptide. Pseudo-prolines are Ser/Thr-derived oxazolidine and Cys-derived thiazolidine derivatives used as protecting groups for serine, threonine, and cysteine. Despite the broad use of SPPS and the advantages there are still inherent problems with solubility and aggregation of the peptide chain. These problems arise from hydrophobic intermolecular aggregation and formation of secondary structure, most often β-sheets. The structural similarity with proline introduces a cis favoured amide bond in the peptide which alters the conformation of the peptide and prevents the formation of β-sheets (see *Figure 3.6*). (Torsten Wöhr et al., 1996) The pseudo-prolines are TFA labile and the oxa-/thiazolidine ring is reverted into the native peptide once cleaved with TFA (see *Figure 3.7*). (Iris Biotech, 2021)

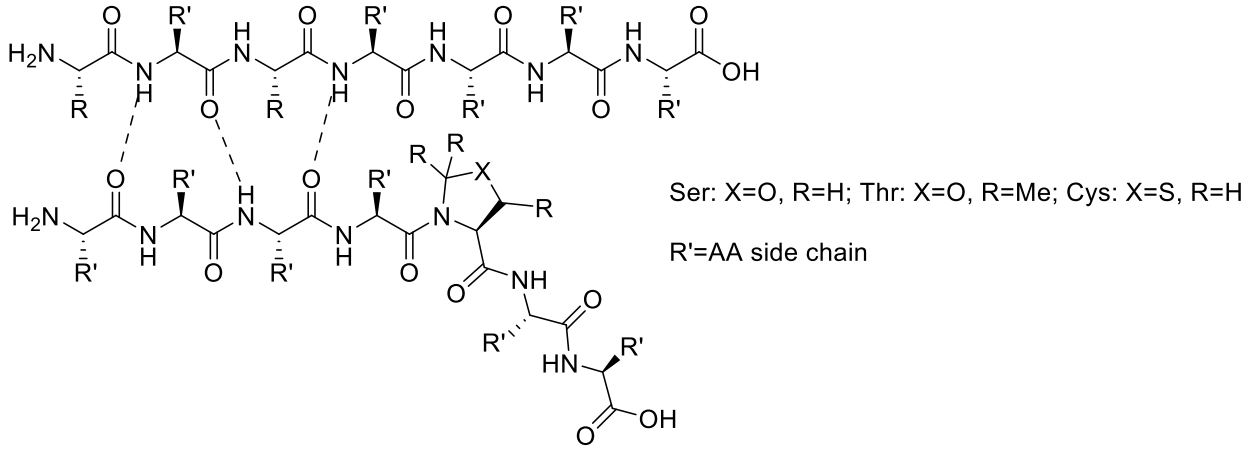

Figure 3.6: β-sheet disruption of pseudo proline. General structure of pseudo prolines and the cis favored amide bond which alters the conformation of the peptide and prevents the formation of β-sheets.

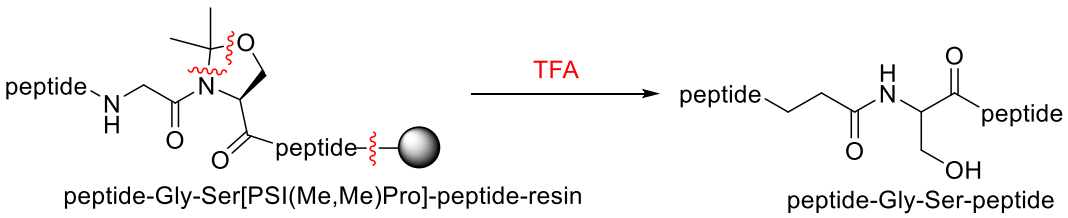

Figure 3.7: TFA cleavage of peptides including pseudo prolines. Structure of a peptide including a Gly-Ser[PSI(Me, Me)Pro] pseudo proline and how it is reverted into the native peptide once cleaved with TFA.

3.1.4 Ninhydrin test

During SPPS it is critical to completely couple the amino acid derivatives to the terminal amino groups. Free terminal amine groups lead to difficulty controlling the synthesis and the peptide will not be pure. If the terminal free amine groups remain the peptide should either be subjected to more coupling reagent or be acetylated. With the use of ninhydrin reagents, it is possible to see whether more than 99% of the amine groups have reacted with the amino acid derivatives. A small sample of resin is placed in a glass tube and 2-3 drops of each of the reagents are added; 0.28M ninhydrin in ethanol, 0.042 M phenol in ethanol and 0.001 M solution of KCN diluted to 100 ml with pyridine. The tube is placed on a heating block at 100ºC. A negative test, that means a complete reaction and no free amines, is indicated by white resin beads and a yellow solution. A positive test is indicated by black resin beads and a blue solution. The reaction only occurs for primary free amines where an imine intermediate is formed which reacts with a second ninhydrin molecule creating a blue conjugate (see *Figure 3.8*). (Kaiser et al., 1970)

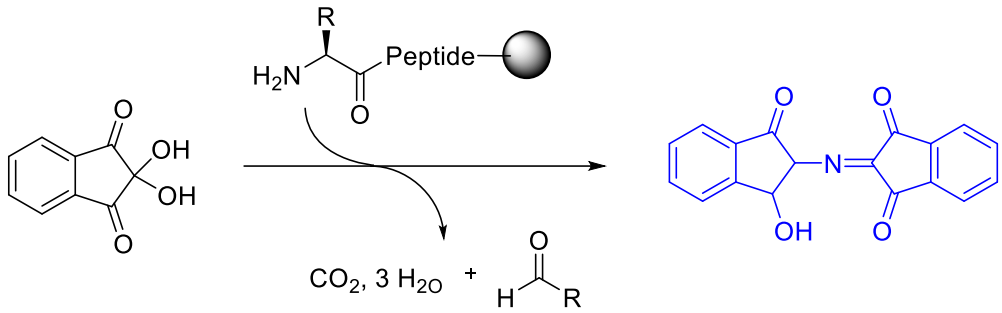

Figure 3.8: Kaiser test. Reaction scheme of a positive kaiser test of a general peptide.

3.1.5 Cyclization

There are several different ways to cyclize peptides, one being thioether formation via cysteine. The nucleophilicity of the cysteine thiol is utilized to form a thioether bond. A reactive moiety, such as chloroacetic acid is coupled to the N-terminus using DIC and oxyma. The thioether linkage is then created via S_N2 displacement of the cysteine with the N-chloroacetylated residue (see *Figure 3.9*). The thioether formation occurs in basic aqueous buffer. (Bechtler and Lamers, 2021) (Kempson et al., 2024)

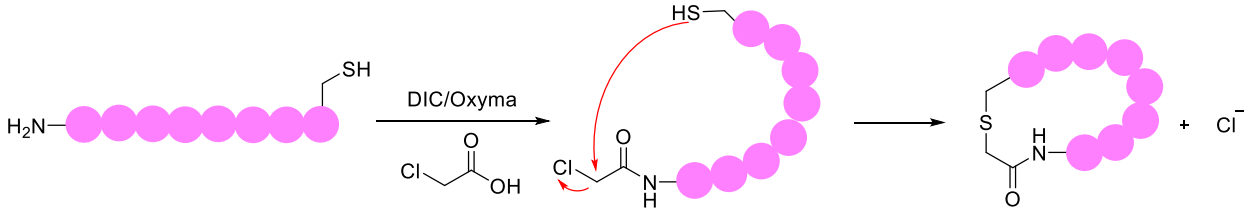

Figure 3.9: Peptide cyclization. Reaction scheme of peptide cyclization via chloroacetic coupling using DIC/oxyma and formation of thioether via cysteine.

3.2 Fluorescence Polarization Assay

Fluorescence polarization (FP) is an assay used to measure binding affinity of small ligands to a larger protein. The technique is based on the observation that fluorescently labelled molecules emit light with a degree of polarization that is inversely proportional to the rate of molecular rotation when excited by polarized light. When a fluorophore is covalently attached to a small ligand (such as a peptide in solution) and excited by polarized light the emitted light will be mostly depolarized. This is due to Brownian molecular rotation of the labelled ligand resulting in reorientation of the fluorophore during the excited state. If the ligand is bound to a protein the fluorophore will reorientate to a lesser extent, resulting in more polarized light being emitted. FP therefore allows for it to be used as a technique to measure ligand binding where the observed polarization in a mixture of ligand and receptor being proportional to the fraction of bound ligand. FP assays have been successfully screened for a wide range of targets and are especially useful when screening for inhibitors of protein-protein interactions. (Moerke, 2009) With the use of FP either saturation or inhibition curves can be determined. For the saturation assay full binding of the labelled probe is achieved by exponentially increasing the protein concentration resulting in polarization of the emitted light (see *Figure 3.10 A*). From the saturation assay the dissociation equilibrium constant (K_d) can be determined. (Prystay, Gosselin and Banks, 2001) In the inhibition assay the binding affinity of unlabelled peptides is tested. The unlabelled peptide is added in exponentially increasing concentrations to a fixed concentration of protein-probe (fluorescently labelled peptide) and incubated. If the peptide binds to the same binding site as the fluorescently labelled protein-probe, this probe will be replaced and cause depolarization of the emitted light (see *Figure 3.10 B*). From this inhibition assay K_i values describing binding affinity can be calculated. (Huang, 2003)

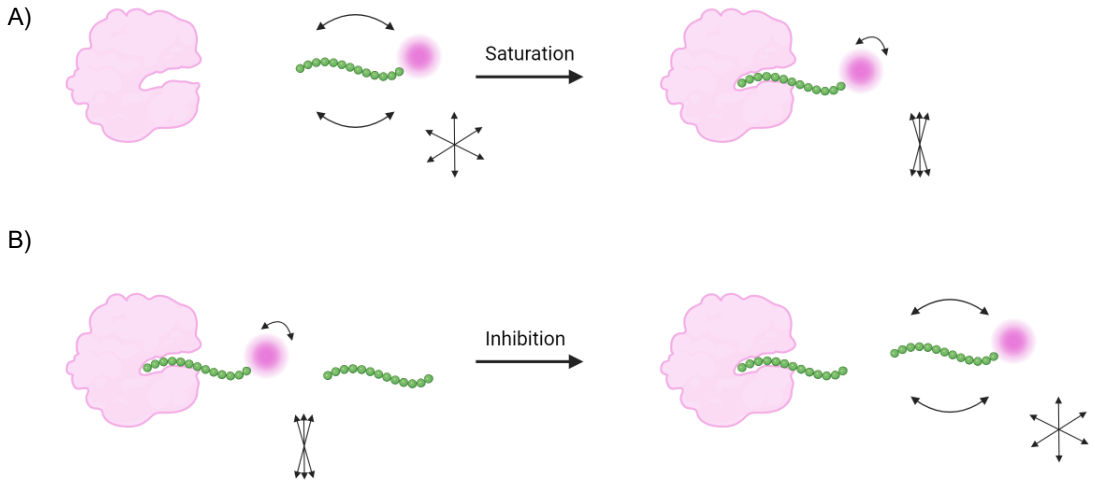

Figure 3.10: Schematic representation of FP: A) Saturation FP where the fluorescently labeled probe (green and magenta) binds to the protein (pink) while being excited by polarized light results in non-polarized light being emitted to different extents. B) Inhibition FP where the peptide (green) inhibits the fluorescently labeled probe (green and magenta) which results in non-polarized light being emitted.

3.3 Plasmin Stability Assay

When ischemic stroke occurs, patients are given tissue plasminogen activator alteplase. Tissue plasminogen activator (tPA) is a serine protease which cleaves peptide bonds in peptides. tPA's primary function is to activate the conversion of plasminogen to plasmin. More specifically it cleaves the zymogen plasminogen at its Arg561-Val562 peptide bond which forms plasmin. Plasmin is the primary enzyme which dissolves blood clots. The alteplase therefore activates the plasmin to dissolve blood clots and restore blood flow. (Jilani and Siddiqui, 2019) However, it was found that Nerinetide is also cleaved by plasmin so that the neuroprotective effect is lost. The peptide was found to be cleaved from the N-terminal Tat domain while keeping the PSD-95 binding C-terminal intact. Plasmin has a similar specificity as tryps which cleaves substrates at C-terminal to arginine or lysine. Plasmin is predicted to cleave Nerinetide after residues 3, 4, 5, 6, 7, 9, 11, and 12 from the N terminus (Mayor-Nunez et al., 2021) (Olsen, Ong and Mann, 2004) It is therefore interesting to measure the stability of the peptides in the presence of plasmin. The peptide is incubated with plasmin and the concentration of the peptide is measured over time with LC/MS.

4 Results and Discussion

In order to evaluate the contribution of each residue in the parent 17-mer cyclic peptide JFL-03, an alanine scan was performed. Alanine scanning is a method of systematic alanine substitution of each residue to determine the functional role of peptide residues. Substitution to alanine is used because it removes the side chain beyond the β carbon while maintaining the main-chain conformation (unlike proline or glycine) (Cunningham and Wells, 1989). The first and last residue in the peptide have not been substituted since they are used in the cyclization of the peptide. Alanine-substituted peptides were synthesized using both manual and automatic SPPS. All successfully synthesized peptides were evaluated for their binding to the PDZ2 domain of PSD-95 using fluorescence polarization (FP). To complement the FP results, predictions of the JFL-03 Ala-variants and their binding to the PDZ2 domain of PSD-95 were performed using AlphaFold. Additionally, the parent 17-mer cyclic peptide JFL-03 was evaluated for its stability against plasmin.

4.1 Synthesis of Peptides FBE_002-005

Synthetic work for this project was initiated by preparing four peptides containing Ala substitutions in positions 2, 3, 4 and 6 (see *Table 4.1*). The peptides were synthesized at a 0.05 mmol scale using a Tentagel R Ram resin. The first five AAs were assembled following a standard manual SPPS protocol using HCTU as coupling reagent. Following a previously reported synthesis strategy for longer peptides, pseudo prolines were incorporated in positions 4-5 or 5-6 using PyBOP as coupling reagent (residues highlighted in red, see *Table 4.1*). The following successful incorporation of the pseudo prolines, the resins were transferred to the PreludeX automated peptide synthesizer (Gyros Protein Technologies, USA) which also uses HCTU as coupling reagent. Following the sequence extension until residue 12, analytical test cleavages (TCs) were performed followed by LC-MS and UPLC analysis (see *Figure 4.1*). The observed m/z values, suggest that the synthesis terminated prematurely due to an *N*-terminal tetramethylguanidinium termination by-product on the N^{α} amine of residue 8 (Arg).
There was likely a system failure concerning the delivery of AA solution for the coupling of residue 9 (Asn), resulting in a coupling cocktail containing too much coupling reagent. In addition, several truncation products were observed for FBE_008, especially a dominant Asn deletion (see *Figure 4.1 D*).

Table 4.1: Gua = N-terminal tetramethylguanidinium termination [((CH3) 2N)2C-Nα-peptide]; exp. = expected m/z value (calculated); obs. = observed m/z value.

Peptide	Sequence	Mass	$[M+H]^+$		$[M+2H]^{2+}$	
			exp.	obs.	exp.	obs.
2	Fmoc-FAGNRIETSF**A**C	1535.69	1536.7	1536.6	768.9	-
	Gua-RIETSF**A**C	1022.53	1023.5	1024.5	512.4	512.4
3	Fmoc-FAGNRIETS**A**TC	1489.67	1490.7	1490.7	745.8	-
	Gua-RIETS**A**TC	976.51	977.5	977.4	489.3	489.3
4	Fmoc-FAGNRIET**A**FTC	1549.70	1550.7	1550.7	775.9	-
	Gua-RIET**A**FTC	1036.55	1037.6	1037.5	519.3	519.4
5	Fmoc-FAGNRI**A**TSFTC	1507.69	1508.7	-	754.6	-
	Fmoc-FAGRI**A**TSFTC	1393.65	1394.5	1394.5	697.8	698
	Gua-RI**A**TSFTC	994.54	995.6	995.8	498.3	498.4

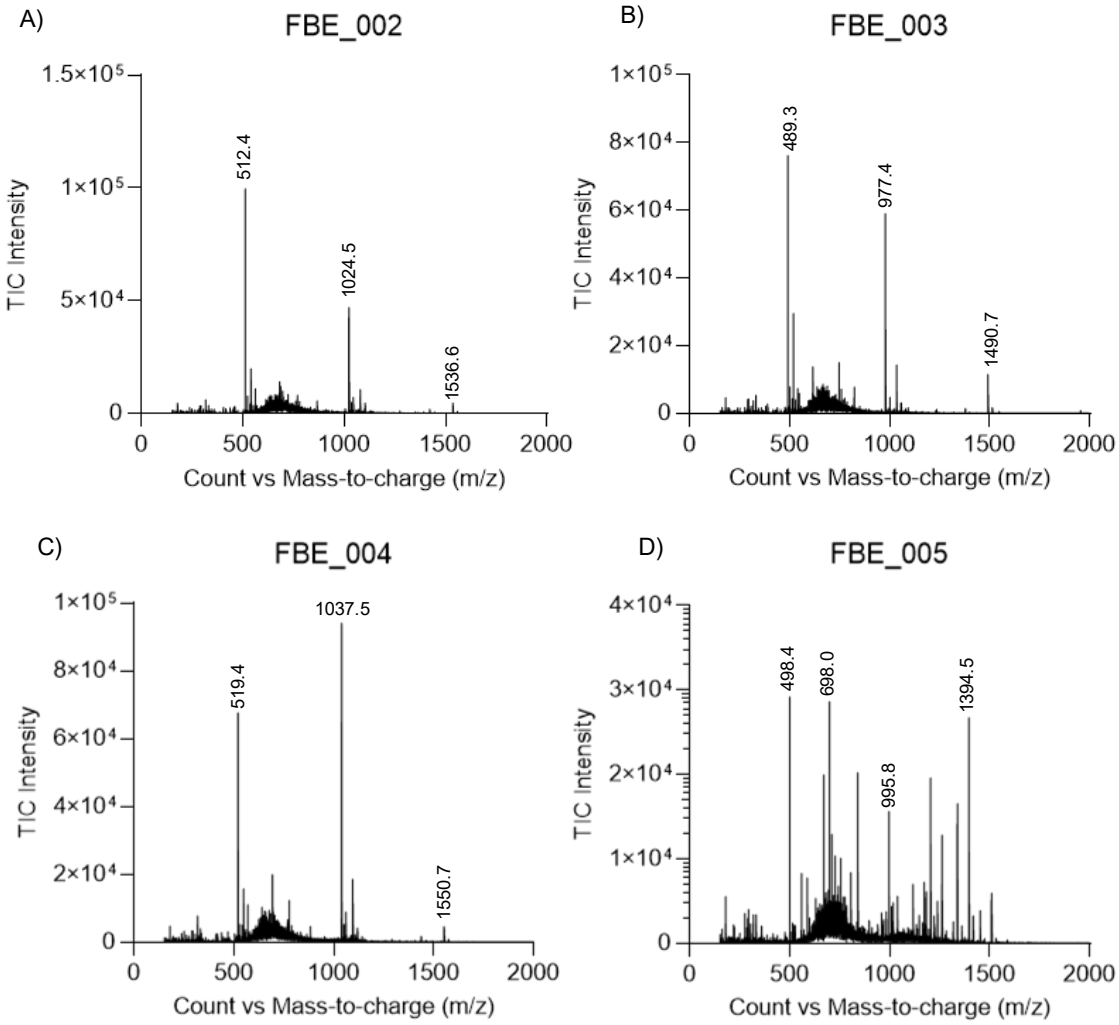

Figure 4.1: LC-MS spectra of peptides FBE_002-005. A) LC-MS of Fmoc protected 12-mer FBE_002 TC. B) LC-MS of Fmoc protected 12-mer FBE_003 TC. C) LC-MS of Fmoc protected 12-mer FBE_004 TC. D) LC-MS of Fmoc protected 12-mer FBE_005 TC.

A common side-reaction for uronium-based coupling reagents like HBTU, HCTU and HATU is the formation of *N*-terminal tetramethylguanidinium by-products. The guadinylation occurs, when the aminium salt of the coupling reagent reacts with the N-terminus of the unprotected peptide to create guanidino derivatives which terminate peptide chain elongation. (Albericio et al., 1998) Often, the termination product forms as a result of excess coupling reagent relative to the AA or due to slow preactivation of the carboxylic acid. (El-Faham and Albericio, 2011). The mechanism of N-terminal guadinylation is shown below (see *Figure 4.2*).

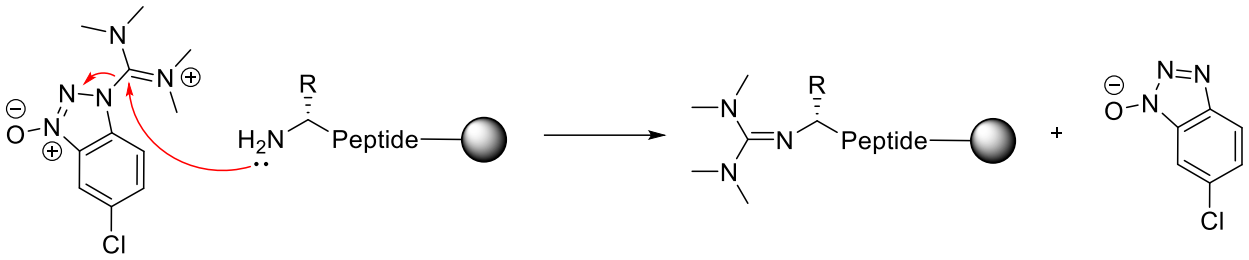

Figure 4.2: N-terminal tetramethylguanidinium formation. Reaction scheme of N-terminal tetramethylguanidinium termination by-product on the Nα amine.

4.2 Synthesis of Peptides FBE_006-010

Further synthetic work for this project was done by preparing four peptides containing Ala substitutions in positions 2, 3, 4 and 6 (see *Table 4.2*, below). The peptides were synthesized at a 0.05 mmol scale using a Tentagel R Ram resin. The first five AAs were assembled following a standard manual SPPS protocol using HCTU as coupling reagent. Pseudo prolines were incorporated in positions 4-5 or 5-6 and 13-14 using PyBOP as coupling reagent (resides highlighted in red, see *Table 4.2*). Following the successful incorporation of the pseudo prolines, the resins were transferred to the Chorus automated peptide synthesizer (Gyros Protein Technologies, USA) which uses DIC/oxyma as coupling reagent. DIC/oxyma was used instead of HCTU to avoid the *N*-terminal tetramethylguanidinium termination by-product. Following the sequence extension until residue 17, analytical test cleavages (TCs) were performed followed by LC-MS analysis (see *Figure 4.3*). The resin was transferred from the Chorus and chloroacetic acid was coupled using DIC/oxyma following a previously reported synthesis strategy. The peptides were then cleaved of the resin using a standard cleavage protocol and solvents were removed by lyophilization. The peptides dissolved in DMSO and subjected to cyclization in a basic buffer composed of acetonitrile and water (1:1 ratio), with a few drops of DIPEA. The resulting cyclic FBE_006 was then purified using HPLC semi-preparative scale, with a gradient from 20% to 50% buffer B over 30 minutes. The observed m/z values, suggest that there was an undesirable formation of side products during deprotection of the 17-mer peptides. All peptides contained an impurity with a mass difference of +51 Da. Based on previous research this impurity was likely the linear chloroacetylated peptide with a piperidine adduct on the C-terminal cysteine. This impurity was observed exclusively after the coupling of chloroacetic acid. Upon cyclization of FBE_006, the impurity appeared to increase, while the yield of the desired peptide diminished. Subsequent purification of FBE_006 resulted in a further reduction of the desired cyclic peptide (see *Figure 4.3 A-C*).

Table 4.2: CAA = N-terminal chloroacetylation, pip = 3-(1-piperidinyl)alanine adduct; exp. = expected m/z value (calculated); obs. = observed m/z value.

Peptide	Sequence	Mass	$[M+H]^+$		$[M+2H]^{2+}$	
			exp.	obs.	exp.	obs.
6	CAA-fIETTFAGNRIETSF**A**C	1980.88	1982.0	1985.2	991.5	992.2
	Cyclic [fIETTFAGNRIETSF**A**C]	1944.90	1945.9	1947.3	973.0	974.3
	CAA-fIETTFAGNRIETSF**A**C+pip	2031.98	2033.0	-	1017.0	1017.4
7	CAA-fIETTFAGNRIETS**A**TC	1934.86	1935.8	1937.2	968.4	968.8
	CAA-fIETTFAGNRIETS**A**TC+pip	1985.86	1986.9	1986.3	993.9	993.7
8	CAA-fIETTFAGNRIET**A**FTC	1994.90	1995.9	1997.3	998.5	998.8
	CAA-fIETTFAGNRIET**A**FTC+pip	2046.00	2047.0	-	1024.0	1023.4
9	CAA-fIETTFAGNRI**A**TSFTC	1952.89	1953.9	1954.3	977.5	978.2
	CAA-fIETTFAGNRI**A**TSFTC+pip	2003.99	2005.0	-	1003.0	-
10	CAA-fIETTFAGNR**A**ETSFTC	1968.84	1968.9	1970.2	985.4	-
	CAA-fIETTFAGNR**A**ETSFTC+pip	2019.95	2021.0	-	1010.9	1010.4

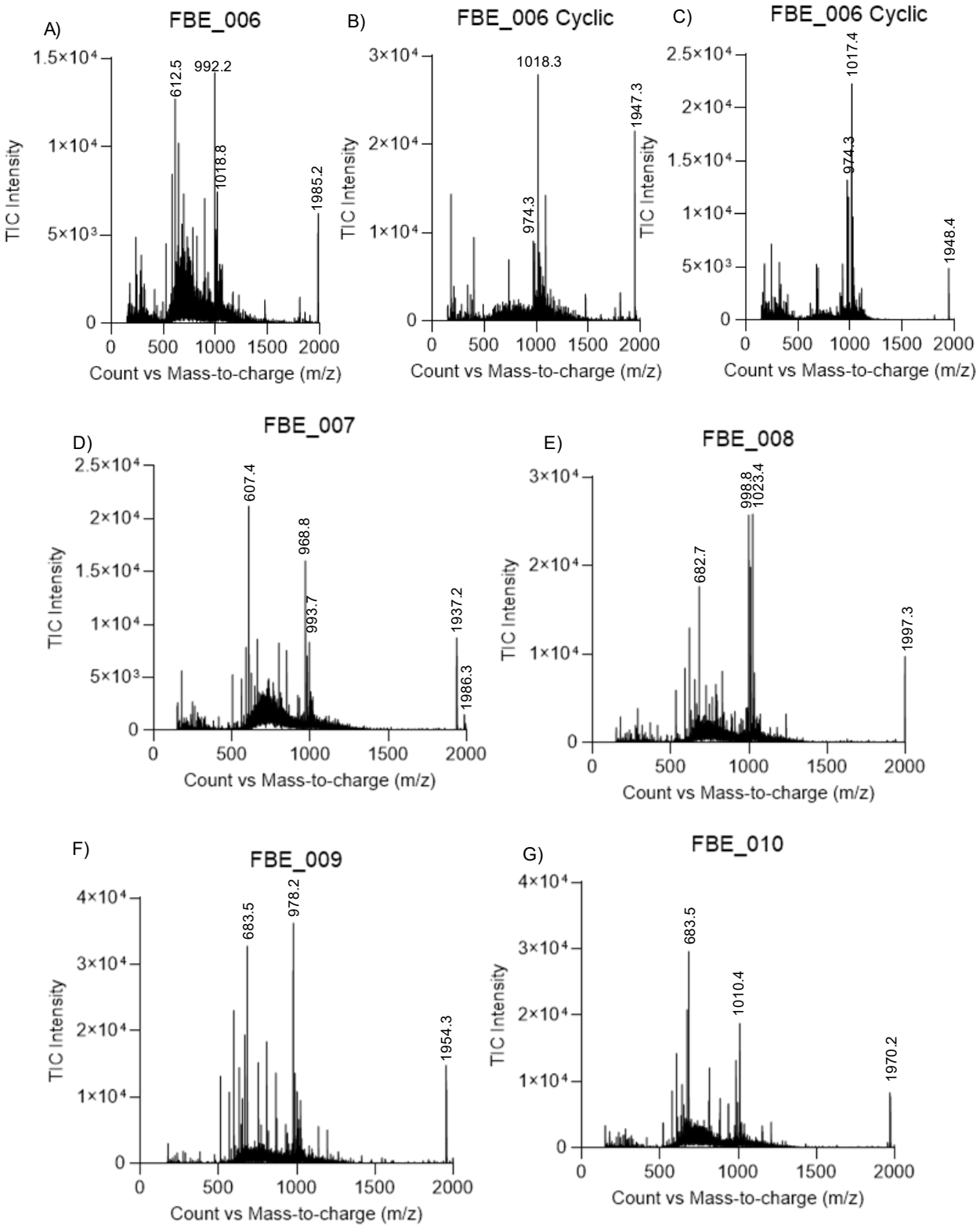

Figure 4.3: LC-MS spectra of peptides FBE_006-010. A) LC-MS of chloro-acetylated 17-mer FBE_006 TC. B) LC-MS of cyclic 17-mer FBE_006 TC. C) LC-MS of a fraction after HPLC purification of cyclic 17-mer FBE_006 TC. D) LC-MS of chloro-acetylated 17-mer FBE_007 TC. E) LC-MS of chloro-acetylated 17-mer FBE_008 TC. F) LC-MS of chloro-acetylated 17-mer FBE_009 TC. G) LC-MS of chloro-acetylated 17-mer FBE_010 TC.

A base-catalyzed elimination of the sulfhydryl-protected side chain followed by a nucleophilic addition to the alkene by piperidine would result in a +51 Da impurity (see *Figure 4.4*). According to previous studies the acidity of the proton of the α-carbon is influenced by the linker connecting the peptide to the resin and the protecting group of the cysteine. (Lukszo et al., 1996) Mthembu et al. (2022) concluded that the use of Fmoc-Cys protected with tetrahydropyran (Thp) and 4-methoxytrityl (Mmt) along with 30% 4-methylpiperidine for Fmoc removal assures minimization of the side reaction.

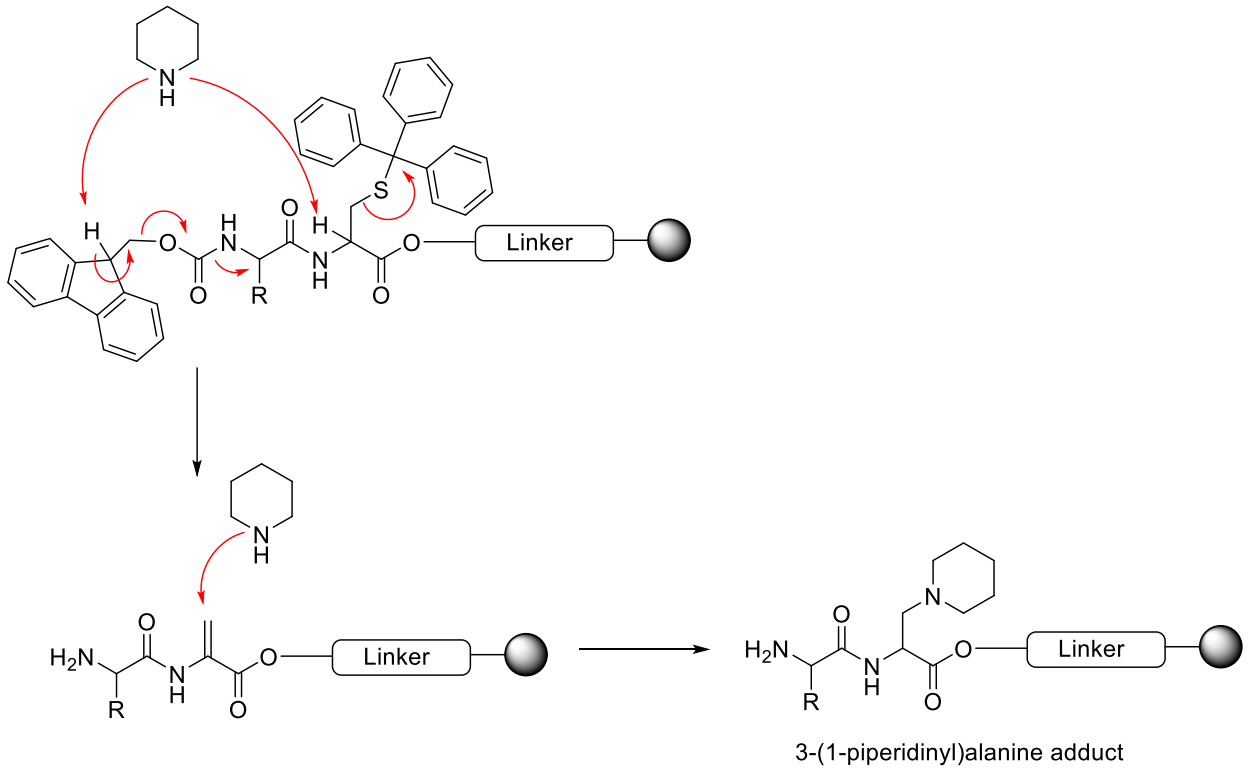

Figure 4.4: 3-(1-piperidinyl)alanine adduct formation. Reaction scheme of base-catalyzed elimination of the sulfhydryl-protected side chain followed by a nucleophilic addition to the alkene by piperidine during Fmoc removal resulting in the 3-(1-piperidinyl)alanine adduct.

4.3 Synthesis of Peptides FBE_011-016

Further synthetic work was done by preparing six peptides containing Ala substitutions in positions 1-6 (see *Table 4.3*, below). The peptides were synthesized at a 0.05 mmol scale using a Tentagel R Ram resin. All AAs were coupled using the PreludeX automated peptide synthesizer (Gyros Protein Technologies, USA) which uses HCTU as coupling reagent. Fmoc-L-Cys(Mmt)-OH was used instead of the previously used Fmoc-L-Cys(Trt)-OH to avoid the 3-(1-piperidinyl)alanine formation. Pseudo prolines were incorporated in positions 4-5 or 5-6 and 13-14 using PyBOP as coupling reagent (resides highlighted in red, see *Table 4.3*). Following the sequence extension until residue 17, analytical test cleavages (TCs) were performed followed by LC-MS and UP-LC analysis. The resin was transferred from the PreludeX and chloroacetic acid was coupled using DIC/oxyma following a previously reported synthesis strategy. The peptides were then cleaved of the resin using a standard cleavage protocol and solvents were removed by lyophilization. The peptides were dissolved in DMSO and subjected to cyclization in a basic buffer composed of acetonitrile and water (1:1 ratio) containing a few drops of DIPEA. The resulting cyclic peptides were then purified using HP-LC semi-preparative scale, with a gradient from 20% to 50% Buffer B over 30 minutes. The obtained purities are found in *Table 4.3* below.

Table 4.3: Sequences and obtained purities of peptides FBE_011-016.

Peptide	Sequence	Purity
11	*Cyclic*[fIETTFAGNRIETSF**A**C]	97%
12	*Cyclic*[fIETTFAGNRIETS**A**TC]	99%
13	*Cyclic*[fIETTFAGNRIET**A**FTC]	98%
14	*Cyclic*[fIETTFAGNRIE**A**SFTC]	97%
15	*Cyclic*[fIETTFAGNRI**A**TSFTC]	96%
16	*Cyclic*[fIETTFAGNR**A**ETSFTC]	96%

4.4 Synthesis of Peptides FBE_017-020

Further synthetic work was done by preparing four peptides containing Ala substitutions in positions 8-11 (see *Table 4.4*, below). The peptides were synthesized at a 0.05 mmol scale using a Tentagel S Ram resin. All AAs were coupled using PreludeX automated peptide synthesizer (Gyros Protein Technologies, USA) which uses HCTU as coupling reagent. Fmoc-L-Cys(Mmt)-OH was used instead of the previously used Fmoc-L-Cys(Trt)-OH to avoid the 3-(1-piperidinyl)alanine formation. Pseudo prolines were incorporated in positions 4-5 and 13-14 using PyBOP as coupling reagent (resides highlighted in red, see *Table 4.4*). Following the sequence extension until residue 17, analytical test cleavages (TCs) were performed followed by LC-MS and UP-LC analysis (see *Figure 4.5*). The resin was transferred from the Chorus and chloroacetic acid was coupled using DIC/oxyma. The peptides were then cleaved of the resin using a standard cleavage protocol and solvents were removed by lyophilization. The peptides dissolved in DMSO and subjected to cyclization in a basic buffer composed of acetonitrile and water (1:1 ratio), with a few drops of DIPEA. Despite the use of Fmoc-L-Cys(Mmt)-OH, the +51 Da impurity was consistently observed in all peptides following the coupling of chloroacetic acid.

Table 4.4: CAA = N-terminal chloroacetylation, pip = 3-(1-piperidinyl)alanine adduct; exp. = expected m/z value (calculated); obs. = observed m/z value.

Peptide	Sequence	Mass	$[M+H]^+$		$[M+2H]^{2+}$		$[M+2H]3^+$	
			exp.	obs.	exp.	obs.	exp.	obs.
17	CAA-fIETTFAGN**A**IETSFTC	1925.83	1926.8	-	963.9	-	642.6	-
	CAA-fIETTFAGN**A**IETSFTC+pip	1976.93	1977.9	1976.7	989.5	988.07	659.9	-
18	CAA-fIETTFAG**A**RIETSFTC	1967.89	1968.9	-	984.6	-	656.9	-
	CAA-fIETTFAG**A**RIETSFTC+pip	2018.99	2020.0	-	1010.5	1010.0	674.0	673.6
19	CAA-fIETTFA**A**NRIETSFTC	2024.91	2025.9	-	1013.5	-	657.9	-
	CAA-fIETTFA**A**NRIETSFTC+pip	2076.01	2077.0	-	1039.0	1038.9	693.0	692.5
20	CAA-fIETT**A**AGNRIETSFTC	1934.86	1935.9	1935.6	968.4	-	645.9	-
	CAA-fIETT**A**AGNRIETSFTC+pip	1985.86	1986.9	1985.7	993.9	993.2	662.9	662.5

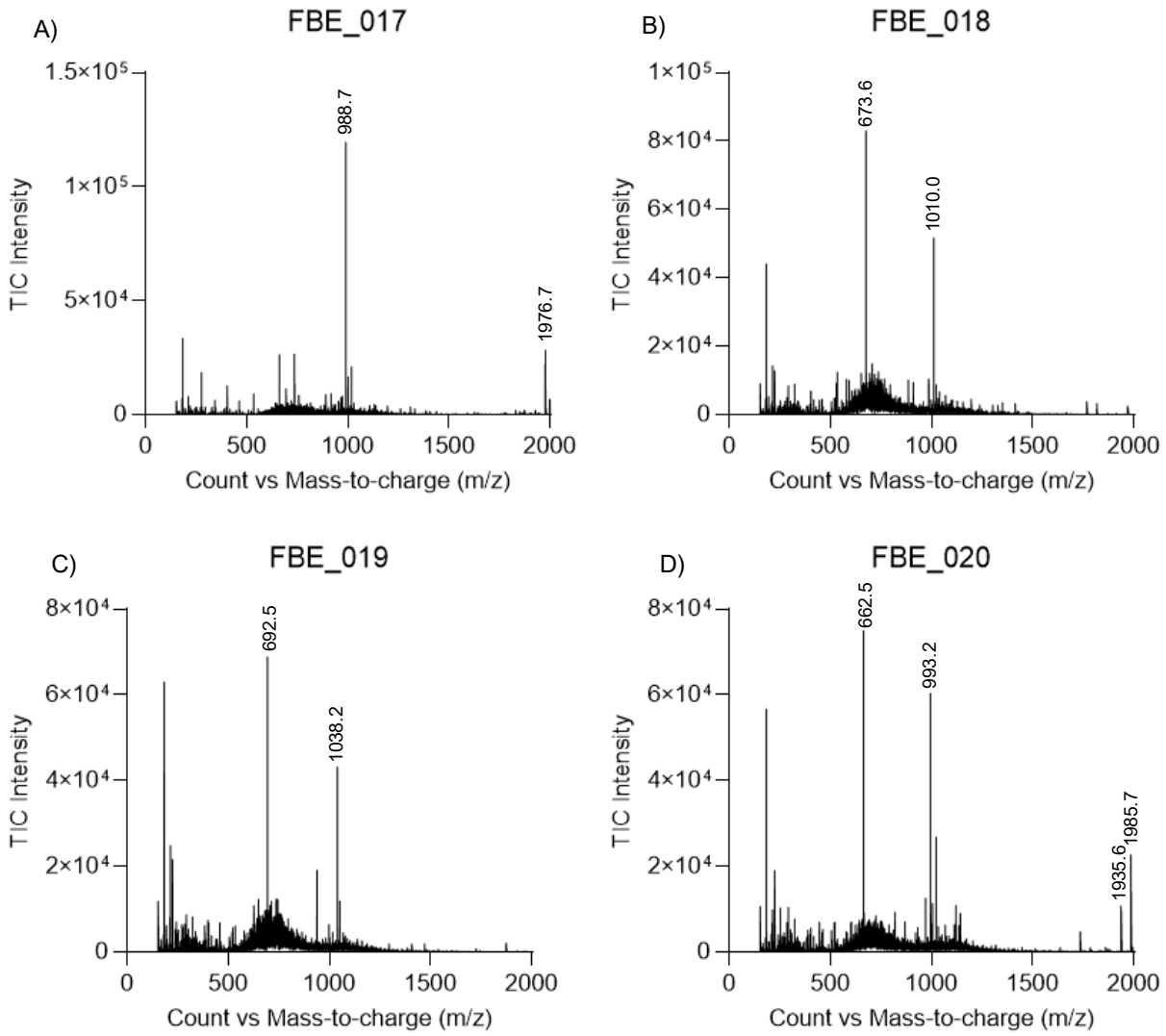

Figure 4.5: LC-MS spectra of peptides FBE_017-020. A) LC-MS of chloro acetylated 17-mer FBE_017 TC. B) LC-MS of chloro acetylated 17-mer FBE_018 TC. C) LC-MS of chloro acetylated 17-mer FBE_019 TC. D) LC-MS of chloro acetylated 17-mer FBE_020 TC.

4.5 Synthesis of FBE_021-024

Synthetic work was done by preparing four peptides containing Ala substitutions in positions 13-16 (see *Table 4.5*, below). The peptides were synthesized at a 0.05 mmol scale using a Tentagel S Ram resin. All AAs were coupled using PreludeX automated peptide synthesizer (Gyros Protein Technologies, USA) which uses HCTU as coupling reagent. Fmoc-L-Cys(Mmt)-OH was used instead of the previously used Fmoc-L-Cys(Trt)-OH to avoid the 3-(1-piperidinyl)alanine formation. Pseudo prolines were incorporated in positions 4-5 or 5-6 and 13-14 using PyBOP as coupling reagent (resides highlighted in red, see *Table 4.5*). Following the sequence extension until residue 17, analytical test cleavages (TCs) were performed followed by LC-MS and UP-LC analysis. Final Fmoc-removal of the 17-mer peptides were done using 10% piperidine and

0.5 M Oxyma to further minimize the formation of the 3-(1-piperidinyl)alanine adduct. The resin was transferred from the PreludeX and chloroacetic acid was coupled using DIC/Oxyma following a previously reported synthesis strategy. The peptides were then cleaved off the resin using a standard cleavage protocol and solvents were removed by lyophilization. The peptides were dissolved in DMSO and subjected to cyclization in a basic buffer composed of acetonitrile and water (1:1 ratio), with a few drops of DIPEA. The resulting cyclic peptides were then purified using HPLC semi-preparative scale, with a gradient from 20% to 50% buffer B over 30 minutes. The obtained purities are found in *Table 4.5* below. Unfortunately, sufficient purity (>95%) of peptide FBE_022 could not be obtained. An impurity with a mass difference of -100 Da was observed in the fractions after purification. This was likely a Thr deletion (see *Table 4.6* and *Figure 4.6*). The Thr deletion likely occurred in the beginning of synthesis (position 2), since the pseudo prolines are building blocks consisting of two AA. If these would not be sufficiently coupled the observed m/z would show deletion of both AT or TS.

Table 4.5: Sequences and obtained purities of peptides FBE_021-024.

Peptide	Sequence	Purity
21	*Cyclic*[fIET**A**FAGNRIETSFTC]	98%
22	*Cyclic*[fIE**A**TFAGNRIETSFTC]	-
23	*Cyclic*[fI**A**TTFAGNRIETSFTC]	99%
24	*Cyclic*[f**A**ETTFAGNRIETSFTC]	98%

Table 4.6: Exp. = expected m/z value (calculated); obs. = observed m/z value.

Peptide	Sequence	Mass	$[M+H]^+$		$[M+H+Na]^{2+}$	
			exp.	obs.	exp.	obs.
22	*Cyclic*[fIE**A**TFAGNRIETSFTC]	1944.90	1945.9	1946.8	984.4	984.5
	Cyclic[fIE**A**TFAGNRIETSFC]	1843.86	1844.9	1845.7	1933.9	1933.9

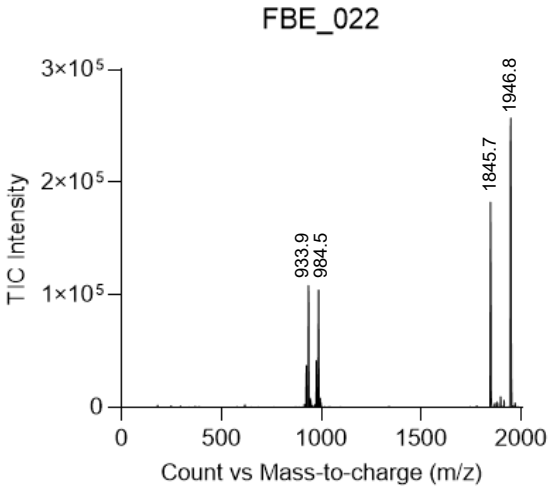

Figure 4.6: LC-MS spectrum of peptide FBE_022. LC-MS of chloro acetylated 17-mer FBE_022 TC.

4.6 Cyclization and purification of FBE_001 (JFL-03)

The wildtype peptide FBE_001 was previously synthesized and provided by Flora Alexopoulou, see sequence in *Table 4.7.* FBE_001 was cyclized and purified following the previously described protocol. The obtained purity can be found in *Table 4.7.*

Table 4.7: Sequence and obtained purity of peptide FBE_001

Peptide	Sequence	Purity
FBE_001	*Cyclic*[fIETTFAGNRIETSFTC]	99%

4.7 Plasmin Stability FBE_001

The stability of FBE_001 against metabolic degradation by plasmin was assessed in an *in vitro* stability assay. Remaining FBE_001 was measured at various time points (0.5, 5, 15, 30, 60 and 120 min) using a single reaction monitoring LC-MS/MS method. Phosphate-buffered saline (PBS) buffer with the peptide was incubated at 37ºC along with reconstituted plasmin from human plasma. As control, the stability of FBE_001 in only PBS buffer was also measured. As depicted in *Figure 4.7*, the peptide demonstrates significant stability, retaining approximately 80% of its initial concentration after 2 hours. Due to this high stability, the half-life cannot be precisely determined, as the concentration does not fall below 50%. Plasmin, similar in specificity to trypsin, cleaves substrates at the C-terminal side of arginine or lysine residues. The FBE_001 lacks lysine residues but contains one arginine residue in position eight. These characteristics, along with the peptide's cyclic structure, likely contribute to its enhanced stability. The resistance against degradation by plasmin is relevant in the context of stroke treatment, as tissue plasminogen activator (tPA) alteplase is the standard of care in the majority of ischemic stroke patients and Nerinetide was reported to suffer significant degradation by plasmin. (Mayor-Nunez et al., 2021)

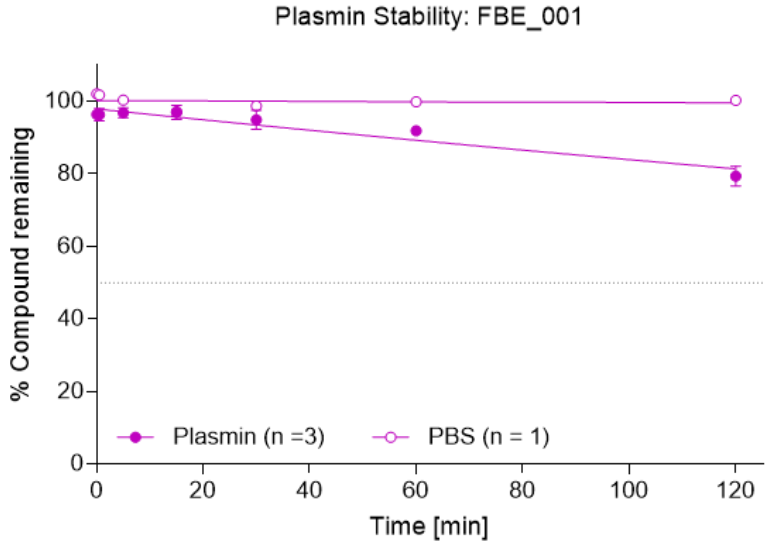

Figure 4.7: Plasmin stability of peptide FBE_001. Plasmin stability over 2h represented as % compound remaining. Data expressed as mean ± SEM (n = 3).

4.8 FP/Affinity determination of JFl-3 and Ala-variants

4.8.1 FP Saturation

In order to determine the binding affinity of unlabelled peptides in a FP inhibition assay, the binding affinity (dissociation constant, K_d value) of a suitable probe needs to be determined. The K_d value of GluN2B probe [(TAMRA)-NNG-EKLSSIESDV] was determined in a saturation FP assay by measuring the polarization (mP) at eleven different concentrations of PDZ2 of PSD-95. The results from the FP saturation assay are shown below (*Figure 4.8 A*). The K_d value was calculated to be 3.6 ± 0.2 µM (n = 3) (*Figure 4.8 B*), which is in good agreement with the literature (K_d = 3.0 ± 0.2 µM). (Bach et al., 2008)

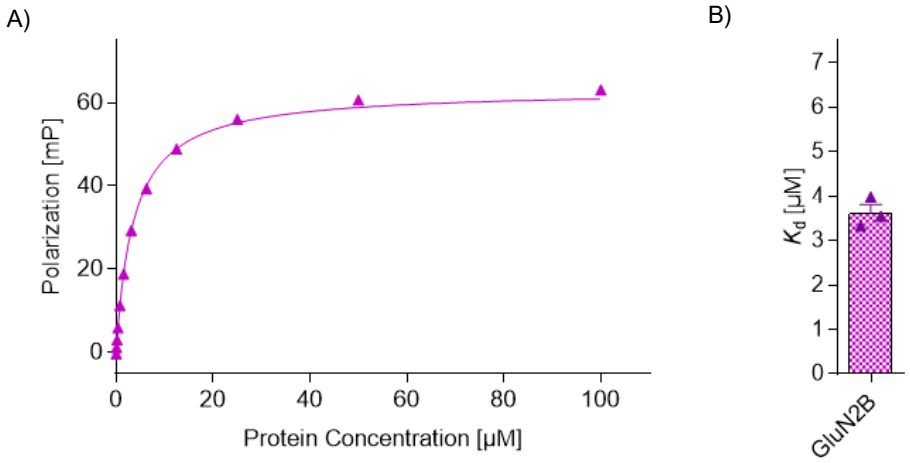

Figure 4.8: FP saturation results. A) FP saturation curve of the TAMRA-GluN2B peptide binding to the PDZ2 domain of PSD-95. Data expressed as mean ± SEM (n = 3). B) Calculated K_d based on FP saturation results. Data expressed as mean ± SEM (n = 3).

4.8.2 FP Inhibition

For the FP inhibition assay, a dilution series containing twelve concentrations of unlabeled peptides was prepared in consistent buffer (5% final DMSO concentration). The protein concentrations for the in-assay probe mix was calculated based on K_d of TAMRA-labelled GluN2B probe (conc. PDZ2 of PSD-95 = 5 µM). The assay was performed by mixing prepared peptide dilutions and probe-protein-mix in a 384-well assay plate. The K_i values were calculated according to Nikolovska-Coleska et al. (2004). Unfortunately, due to synthesis problems and time limits, a complete Ala-scan of JFL-03 could not be prepared. However, nine out of fifteen peptides were tested. The normalized polarization for all tested peptides is shown in *Figure 4.9*. Interestingly, the various Ala substitutions had different effects on the binding of JFL-3 to PDZ2 of PSD-95. The corresponding K_i values are summarized in *Table 4.8*.

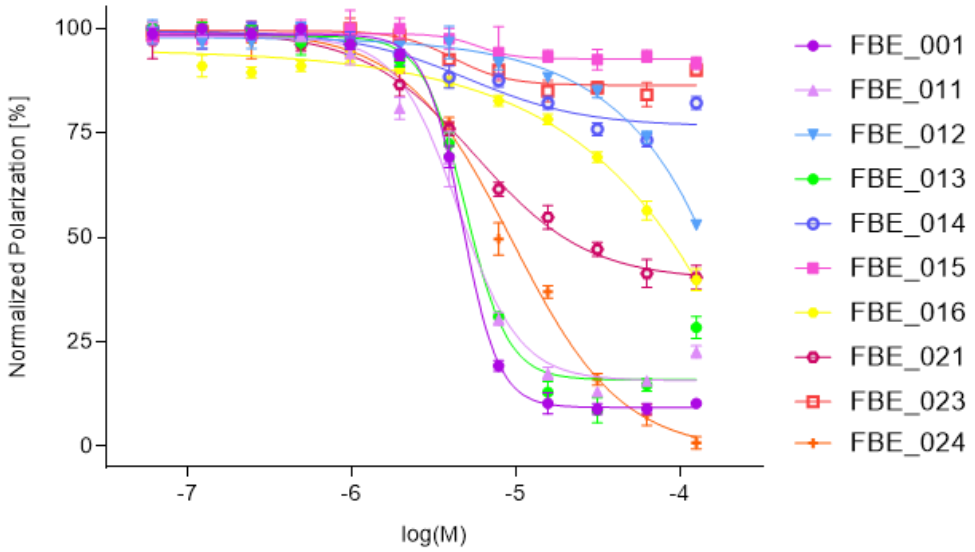

Figure 4.9: FP inhibition results of the partial JFL-3 Ala-scan. FP inhibition of peptides FBE_001 and FBE_011-024 using the TAMRA-GluN2B probe and PDZ2 domain of PSD-95. Data expressed as mean ± SEM (n = 3).

The K_i value for each peptide was calculated from the inhibition assay data (see *Table 4.8.* and *Figure 4.10*). Peptides FBE_014 , FBE_015 and FBE_023 shows the highest K_i values and can be considered to have no binding affinity for PDZ2 of PSD-95 (K_i value >125 µM). Further on, FBE_016 and FBE_020 also show low affinity and high K_i values ranging between 70 and 100 µM. Peptides FBE_011, FBE_013, FBE_021 and FBE_024 show least change in K_i values with FBE_011 exhibiting only a 5-fold loss in binding affinity (K_i = 2.6 µM).

Table 4.8: K_i values of peptides calculated from FP inhibition assay. Affinity = fold change of K_i based on FBE_001.

Peptide	Sequence	Mutation	K_i ± SEM [µM]	Affinity
1	*Cyclic*[fIETTFAGNRIETSFTC]	None	0.53 ± 0.03	
11	*Cyclic*[fIETTFAGNRIETSF**A**C]	T16 → A	2.6 ± 0.5	5x lower
12	*Cyclic*[fIETTFAGNRIETS**A**TC]	F15 → A	98 ± 2	185x lower
13	*Cyclic*[fIETTFAGNRIET**A**FTC]	S14 → A	3.0 ± 0.07	7x lower
14	*Cyclic*[fIETTFAGNRIE**A**SFTC]	T13 → A	125 ± 0.0	None
15	*Cyclic*[fIETTFAGNRI**A**TSFTC]	E12 → A	125 ± 0.0	None
16	*Cyclic*[fIETTFAGNR**A**ETSFTC]	I11 → A	70 ± 5	132x lower
21	*Cyclic*[fIET**A**FAGNRIETSFTC]	T5 → A	8.1 ± 0.7	15x lower
23	*Cyclic*[fI**A**TTFAGNRIETSFTC]	E3 → A	125 ± 0.0	None
24	*Cyclic*[f**A**ETTFAGNRIETSFTC]	I2 → A	5.7 ± 0.2	11x lower

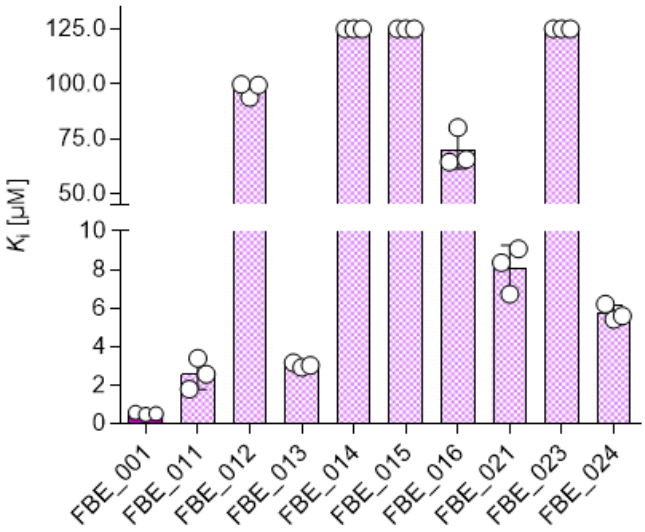

Figure 4.10: K_i results. Calculated K_i values from FP inhibition results according to Nikolovska Coleska et al. (2004). Data expressed as mean (n = 3).

For class I PDZ domains that canonically bind ligands, C-terminal recognition motif is T/S-X-Ψ (X being any amino acid, and Ψ being a hydrophobic residue). The T/S in position -2 forms a hydrogen bond with the imidazole side chain of the His in αB. The PDZ2 domain also binds non-canonically to the nNOS protein where position 0 is a phenylalanine buried in the hydrophobic pocket. (Christensen et al., 2019) Previous mutational scan of a cyclic nNOS peptide performed in the Strømgaard group showed importance of the 'TTF' motif in the β-strand for binding to the PDZ2. The authors also showed importance of the 'G' and 'P' in the β-hairpin loop and 'T' in the antiparallel strand (see *Table 4.9*). (Balboa et al., 2022) Flora Alexopoulou performed a RaPID deep mutational scan of the JFL-03 peptide and found that mutations in most positions, including the 'TTF' motif, were detrimental for binding (see highlighted residues in *Table 4.9*). It is postulated, that JFL-03 adopts a similar antiparallel β-strand structure as the nNOS peptide when binding to PDZ2. Alexopoulou also found that mutations in positions 6, 7, 8 and 16 were more tolerated. Unfortunately, positions 6, 7, 8 were not probed in the Ala-scan. The substitution of T16 to A appears to be more tolerated compared to the other substitutions, which is in agreement with the previous RaPID deep mutational scan results. Based on the results of this Ala-scan, positions E3, E12 and T13 appear to be most importance for binding to PDZ2. I11 and F15 are also of high importance, as the peptides show low affinity for the protein (K_i values between 70 and 100 µM). The least important among the investigated residues are I2, T5, S14 and T16 representing on a 5- to 15-fold loss in affinity (see *Table 4.9*). The tolerated S14 and T5 to A mutation agrees with canonical binding of PDZ class I domains which recognises the T/S-X-Ψ motifs since the mutation does not affect the binding as much as other mutations. It also agrees with the non-canonical binding of the nNOS β-hairpin structure where phenylalanine which buries itself in a hydrophobic binding pocket of the PDZ. Hypothetically there could be two binding motifs in the cyclic JFL-03 peptide: 'TTF' and 'TSF' and they both match for the canonical and non-canonical binding.

Table 4.9: Sequence alignment of nNOS cyclic peptide with JFL_03/FBE_001. AAs in bold indicate critical residues for binding to PDZ2. (Alexopoulou, 2022) Residues in red have not been evaluated.

Peptide	Length (AA)	Sequence
nNOS	23	^{105}TH**LETTF**T**G**DGT**P**K**T**IRVTQ^{124}
JFL-03	17	f**IETTF**AGN**RIETSF**TC
FBE_001	17	fI**E**T*TFAGNR***IET**S**F**TC

4.9 Alpha Fold

To complement the FP results, simulations of the JFL 03 (FBE_001) Ala-variants and their binding to the PDZ2 domain of PSD-95 were performed using AlphaFold. However, it is important to note that the alignments provided by AlphaFold are only predictions, as AlphaFold cannot model macrocyclic peptides. Because of this there is a gap in the predicted structure. The PDZ2 domain used is based on an existing crystal structure (PDB: 3ZRT). (Bach et al., 2012) In *Figure 4.11 A* the predicted binding of the nNOS β-hairpin peptide (blue) to synthropin-PDZ (green). (Hillier, 1999) The nNOS peptide adopts an antiparallel β-strand fold and binds in a non-canonical fashion. The prediction suggests that the '^{108}ETTF^{113}' motif is crucial for binding and that nNOS adopts a β-hairpin loop. The 'ETT' stretch of residues forms hydrogen bonds with residues in the PDZ2 domain, while F112 lies in the binding pocket between βB and αB of the PDZ2 domain. Additionally, the His70 residue in the αB helix of PDZ2 forms a hydrogen bond with the T110 residue at position -2 from the hydrophobic residue F112 in nNOS.

In *Figure 4.11 B* the nNOS peptide is aligned with the RaPID derived peptide FBE_001 (magenta)and its predicted binding to PDZ2 of human PSD-95 PDZ1-2 (green). Interestingly, FBE_001 appears to adopt a similar structure to the nNOS peptide. However, the peptide's orientation in the binding pocket is rotated by 180° (see orientation of the peptide termini). For FBE_001, the '^{11}ETSF^{16}' motif faces inward towards the binding pocket, resulting in the β-hairpin loop turning the opposite way. The 'ETSF' forms hydrogen bonds with residues in the PDZ2 domain, while F15 lies in the binding pocket between βB and αB of the PDZ2 domain. The T13 forms a hydrogen bond with the His70 residue in the αB helix of PDZ2 at position -2 from the hydrophobic residue F15 in nNOS.

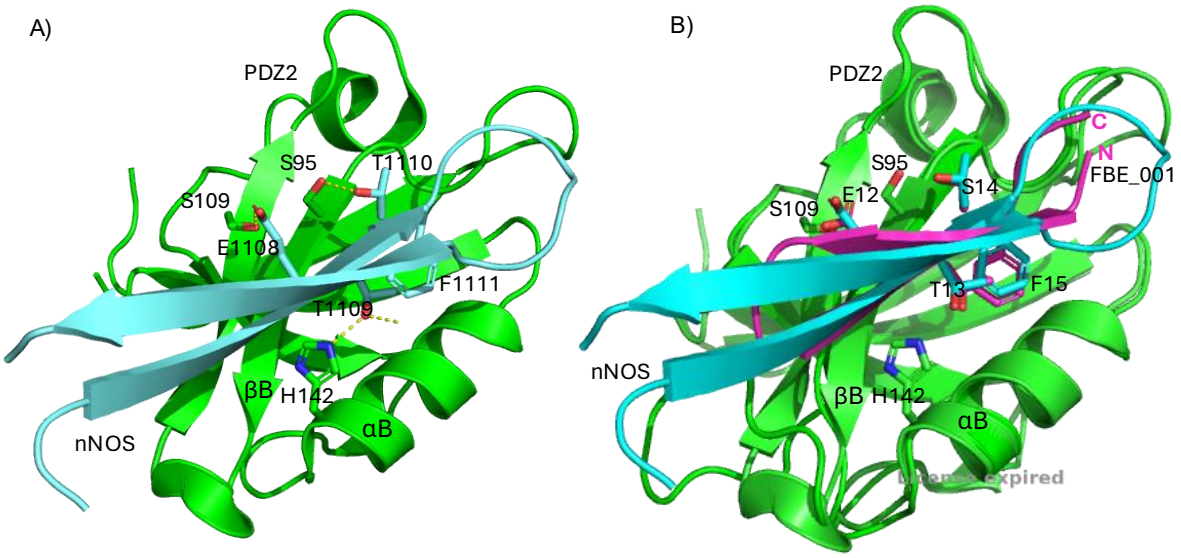

Figure 4.11: Secondary structure of PDZ2/nNOS and PDZ2/FBE_001. A) Cartoon representation of the X ray crystal structure of syntrophin-PDZ/nNOS (green/blue) (PDB ID: 1QAV) using AlphaFold. Hydrogen bonds between side chains of PDZ2 and nNOS are shown in yellow. B) Cartoon representation of the X ray crystal structure of syntrophin-PDZ/nNOS (green/blue) overlapping FBE_001/PDZ2 (green/magenta) using AlphaFold (PDB ID: 3ZRT).

When predicting the substituted Ala-scan peptides of FBE_001 with AlphaFold, the peptide seems to bind to the PDZ2 in a similar way as nNOS peptide (see *Figure 12 A-I*). When replacing residues in the '^{11}ETSF^{16}' motif with alanine, it seems that the '^{2}ETTF^{7}' motif faces the protein, similar to nNOS (e.g. *Figure 4.12 A-B*). Peptides FBE_012, FBE_014, FBE_015, all exhibiting significantly reduced binding affinity in the FP inhibition assay, are predicted to bind in the same pose as the nNOS peptide, indicating that the '^{11}ETSF^{16}' motif might be preferred oved the '^{2}ETTF^{7}' motif. Only FBE_013 (S14A substitution) faces to the opposite way of nNOS, when substituting the '^{11}ETSF^{16}' motif. FBE_013 also shows rather high affinity for the protein, suggesting that the S14 in the '^{11}ETSF^{16}' motif is not of most importance and the peptide still binds in a similar fashion as FBE_001. This is unexpected, since S14 is predicted to form hydrogen bonds with residue S95 in PDZ2, similar to the nNOS peptide in *Figure 4.11* B where T1110 (in nNOS) and S95 (in PDZ2) form a hydrogen bond. However, it does align with the canonical binding of T/S-X-Ψ where the X can be any residue. It also aligns with the non-canonical binding where the hydrophobic residue at position 0 is a phenylalanine, in this case F15 or F5, buries itself in a hydrophobic binding pocket of the PDZ2.

When substituting residues E3 and T5 the '^{11}ETSF^{16}' motif faces the protein for both peptides. However, the E3A substitution still show no affinity for the protein in the FP inhibition assay. This implies that both motifs are important for binding. The FBE_021 (T5A substitution) shows rather high affinity for the protein similar to FBE_013 (S14A substitution). Again, this agrees with both the canonical and non-canonical binding to PDZ2.

The peptides also seem to form the antiparallel β-sheets to different extents. For FBE_011 the β-sheets are shorter and for FBE_014 only one β-sheet is formed (see *Figure 4.12 A* and *D*). This

implies that T16 and T13 are important for the β-sheet formation and potentially form intermolecular hydrogen bonds stabilizing the antiparallel β-sheet conformation.
Notable, residues F6 and F15 are always buried inside the binding pocket which is reasonable since proteins fold into a structure with a hydrophilic surface and hydrophobic core. (Wu and Tian Yow Tsong, 2013) This also agrees with the non-canonical binding of β-hairpin loops to PDZ2.

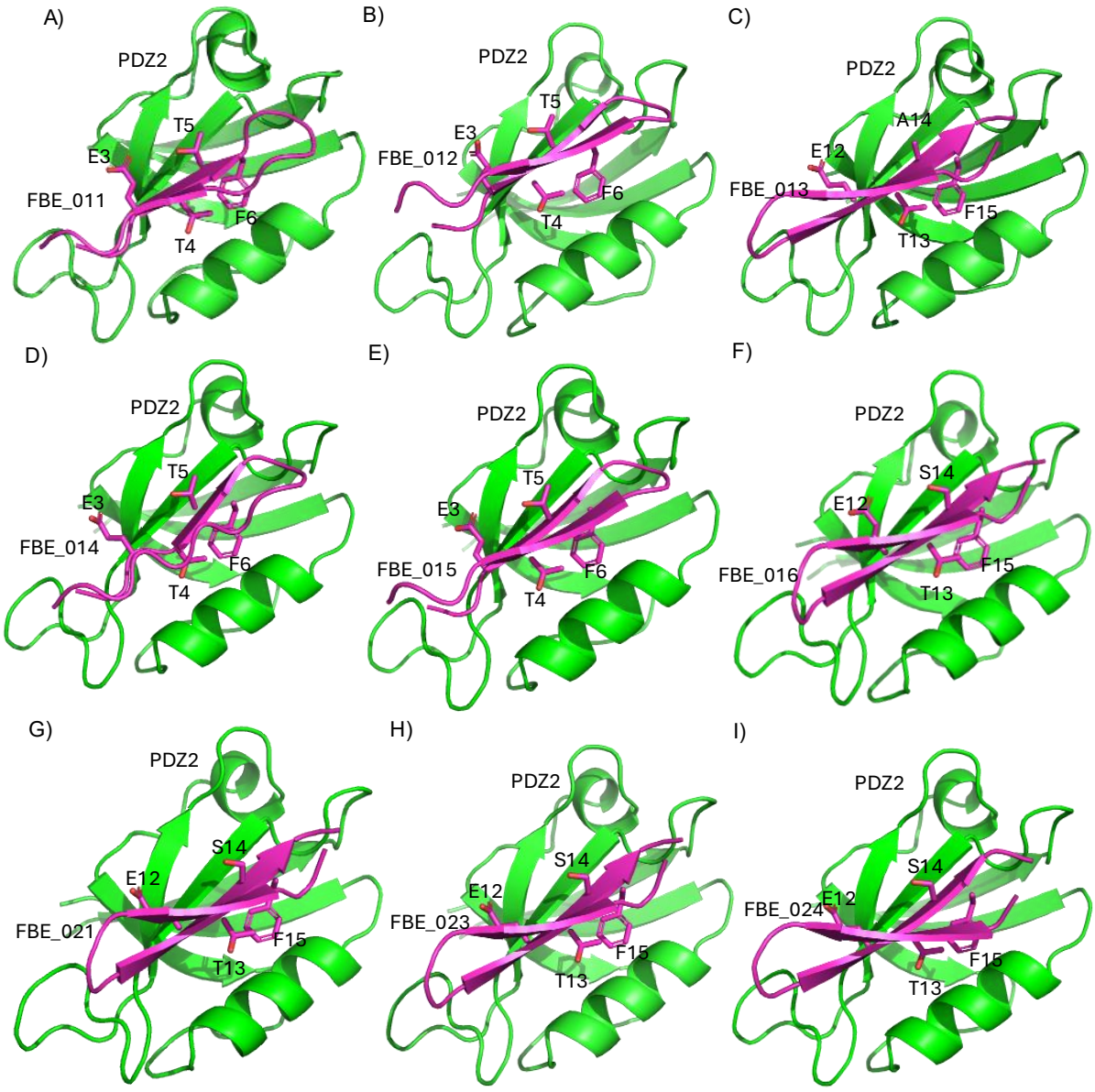

Figure 4.12: Secondary structure of PDZ2/FBE_011-016 and PDZ2/FBE_022-024. Cartoon representation of the X ray crystal structure of PDZ2 (green) (PDB ID: 3ZRT) and the predicted binding of A) FBE_011 B) FBE_012 C) FBE_013 D) FBE_014 E) FBE_015 F) FBE_016 G) FBE_022 H) FBE_023 I) FBE_024 (magenta) using AlphaFold.

Finally, it is possible that the peptides bind two PDZ2 domains at the same time. Since the peptide is cyclic and seems to have two binding motifs, they could each bind to the protein at the same time. They contain the T/S-X-Ψ motifs in an inverted orientation, where hypothetically two PDZ2 domains could bind. Both binding motifs also match the non-canonical binding and based on the predictions the peptide seems to be able to insert itself into the binding pocket in two different ways. This would explain why changing both motifs 'ETTF' and 'ETSF' individually leads to a significant increase in K_i values and drop in affinity.

5 Conclusions and Future perspectives

In this project, a detailed structure-activity relationship (SAR) investigation into the binding of FBE_001 to the PDZ2 domain of PSD-95 was initiated. Unfortunately, a complete Ala-scan could not be performed due to the difficulties in peptide synthesis and time-limitations. This makes it impossible to assess the contribution of each of the residues and their binding to the PDZ2 of PSD-95. However, nine out of the initially planned fourteen residues have been evaluated. Based on the FP results of the alanine substituted peptides it can be conclude that E3, E12 and T13 are the most important residues among the evaluated for binding to the PDZ2. Furthermore, it can be concluded that I11 and F15 are also highly important for binding and that I2, T5, S14 and T16 are less important for the binding to PDZ2. Finally, the peptide FBE_001 appears to be metabolically stable when tested in a plasmin stability assay.

For future work, the Ala-scan should be completed. This will give more insights into the contributions of each residue and their impact on binding. It would be of interest to have FP results of mutations of the whole '^{2}ETTF^{7}' motif and on the residues in the β-hairpin loop. It would allow us to possibly draw more conclusions around the different motifs that seems to bind the protein. Ala substitutions of the residues in the loop would give us information on the importance of the conformation and eventually the structure of the peptide.
Furthermore, additional position scans such as *N*-methylated AA and D-AA scans, offer possible ways to to identify which intramolecular hydrogen bonds are important for the peptide's structure and function and to assess the importance of stereochemistry at each position. *N*-methylated AAs could also increase the membrane permeability of the peptide, another important property of the peptide to investigate.
Finally, according to Tanada et al. (2023) cyclic peptides containing 9-11 AAs are optimal scaffold to eventually achieve cellular uptake. Therefore, the next step would be to miniaturize the 17-mer lead peptide by removing the less important residues. This would possibly increase the cell permeability, which is highly desirable targeting an intracellular protein like PSD-95.
The insights into the structure-affinity relationship of macrocyclic peptides targeting the PDZ2 of PSD-95 gained from this study can be further used to develop effective therapeutic approaches targeting brain damage caused by ischemic strokes.

6 Experimental

6.1 General Methods

6.1.1 LC-MS

Mass spectra were obtained with an Agilent 6470 Quadrupole LC/MS System (Agilent Technology, Germany) using AJS-ESI ionization technology (Jet Stream Technology Ion Source, Electron Spray Ionization). Samples were run on a reversed-phase C18 column (EC-C8, 2.1 x 50 mm, 1.9u) (Agilent Technology, Germany) with a gradient of 5-95% buffer B in buffer A over 3 min. (A: H2O/TFA, 99.9:0.1 % and B: MeCN/TFA 99.9:0.1 %).

6.1.2 UPLC

Purity of peptides was determined with ultra-performance liquid chromatography (UPLC) (Waters Acquity, US). The samples were run on a reversed-phase C18 column (Acquity UPLC BEH C18, 1.7 x 50 mm) (Waters, US) with a gradient of 5-95% buffer B in buffer A over 7 min (A: H2O/MeCN/TFA 95:5:0.1 % and B: H2O/MeCN/TFA 5:95:0.1 %). Purity was then determined in terms of percentage from area under curves (AUCs) in the chromatograms (λ =214 nm).

6.2 Solid-phase Peptide Synthesis

6.2.1 Manual SPPS

Peptides were manually synthesized using the Fmoc-strategy in a reaction vessel on a 0.05 mmol scale. Tentagel R Ram resin or Tentagel S ram resin was used. Before use, the resin was left to swell in DMF for 15 minutes before use. For couplings Fmoc-protected amino acids preactivated with HCTU and DIPEA (resin/AA/HCTU/DIPEA, 1:4:4:4 equivalents) in 1 ml DMF were used and added to the resin. The reaction was left to shake at room temperature (rt) for minimum 1h. The resin was then washed 3x with DMF. Fmoc-deprotection was then performed using 3 ml 20% piperidine in DMF for 2x3 min. After the resin was washed 3x with DMF before the next coupling.

6.2.2 Automated SPPS

Automated SPPS was performed on a PreludeX, induction heating assisted peptide synthesizer (Gyros Protein Technologies, Tucson, AZ, USA). Peptides were synthesized using the Fmoc-strategy in a 10 ml glass reaction vessel on a 0.05 mmol scale. Fmoc-AAs were preactivated with HCTU and DIPEA (AA/HCTU/DIPEA, 1:1:2 equivalents) and added in a 3-fold compared to the loaded resin. Couplings were performed 3x for 5 minutes, shaking at 50ºC. Deprotection was carried out 2x for 2 minutes by adding 20% piperidine in DMF and shaking at rt or 50ºC.

Automated SPPS was also performed on a Chorus, induction heating assisted peptide synthesizer (Gyros Protein Technologies, Tucson, AZ, USA). Peptides were synthesized using the Fmoc-strategy in a 10 ml glass reaction vessel on a 0.05 mmol scale. Fmoc-AAs were preactivated with DIC and oxyma (AA/DIC/oxyma, 1:2.5:2.5 equivalents) and added in a 3-fold compared to the loaded resin. Couplings were performed 3x for 5 minutes, shaking at 50°C. Deprotection was carried out 2x for 2 minutes by adding 20% piperidine in DMF and shaking at rt or 50°C.

6.2.3 Monitoring Coupling Reactions

To monitor the coupling reactions Kaiser tests and test cleavages were sporadically performed. For the Kaiser test a small amount of resin was transferred to a glass tube and two drops of each of the reagents 80% phenol in ethanol, KCN in H_2O/pyridine and 6% ninhydrin in ethanol were added. The tube was placed on a heating block (90°C) for 5 minutes and the colour change was monitored. Test cleavages were performed by transferring a small amount of resin to an Eppendorf tube. 250 µl of cleavage solution (Tips/H_2O/TFA, 2.5:2.5:95 %) was added and the Eppendorf tube was left in a water bath (50°C) for 5 minutes. The peptide was then precipitated using ice-cold diethyl ether, resolubilized in buffer A:B containing H2O/MeCN/TFA (A: 95:5:0.1 % and B: 5:95:0.1 %), filtered and analyzed with UPLC and LCMS.

6.2.4 Coupling of Pseudo Prolines

Fmoc-deprotection was performed using 3 ml 20% piperidine in DMF for 2x3 min. Afterwards the resin was washed 3x with DMF. Pseudo prolines preactivated with PyBOP and DIPEA (resin/pseudo proline/PyBOP/DIPEA, 1:2:2:4 equivalents) in 1.5 ml DMF were used and added to the resin. The reaction was left to shake at rt or 50°C for 1h.

6.2.5 Chloroacetylation of Peptides

Fmoc-deprotection was performed using 3 ml 20% piperidine in DMF for 2x3 min. Afterwards the resin was washed 3x with DMF. Chloroacetic acid preactivated with oxyma and DIC (resin/CAA/oxyma/DIC, 1:5:7.5:5 equivalents) in 2.5 ml DMF were used and added to the resin. The reaction was left to shake at rt for 30 minutes.

6.2.6 Cleavage of Peptides

For final cleavage of peptides, they were transferred to a 10 ml glass vial. 6 ml of cleavage mixture (DODT/Tips/H_2O/TFA, 1.25:2.5:2.5:93.75 %) was added and the reaction was left to shake for 2h at rt. Afterwards, the resin was removed by filtration and the peptide was precipitated with ice-cool diethyl ether, resolubilized in buffer A:B (1:1), freeze dried and purified using preparative HPLC.

6.2.7 Purification of Peptides

Purification of peptides was performed by preparative reversed-phase HPLC (Waters, Milford, MA, USA). Purifications were done using a C18 column (YMC-Pack ODS-A, S-5 µm, 250 x 20.0 mm) (YMC Europe GMBH, Germany) and a linear gradient of buffers containing H2O/MeCN/TFA (A: 95:5:0.1 % and B: 5:95:0.1 %). The quality of the fractions, selected based on absorbance at 214 nm, was determined using UPLC and LCMS. Subsequently, fractions with purity above 95% were combined and solvents were removed on freeze dryer.

6.3 Fluorescence Polarization Assay

Binding affinities were determined in a flat bottom black 384well plate (Corning Life Science) using a plate reader (Tecan Safire2, Cisbio). All experiments were conducted in 150 mM NaCl, 25 mM HEPES, 1 mM TCEP, 1% BSA, pH 8.0 at 25°C and the fluorescence was measured at excitation/emission wavelength of 530/580 nm. The instrumental Z factor was adjusted to maximum fluorescence and the G factor was calibrated to give an initial millipolarization of 20 mP. Either FP assays were performed as saturation or competition experiments using the TAMRA-GluN2B peptide (TAMRA)-NNG- EKLSSIESDV as probe at a concentration of 50 nM and the PDZ2 domain of PSD95 (PSD95-PDZ2-7xHis, WT) as protein binding partner.

6.3.1 Saturation Assay

For FP saturation experiments (determination of K_d values), the polarization was measured at eleven different protein concentrations prepared via a 1:1 dilution series (max. protein concentration in assay: 100 µM). All experiments were performed in triplicate and the data was fitted to a one-site binding model (B max constrain: 63.1 mP) using GraphPad Prism (10.2.3).
For competition experiments (determination of K_i values), a preformed complex of PSD95-PDZ2 (10 µM)/TAMRAGluN2B was outcompeted with unlabeled peptides at eleven different concentrations (max. peptide concentration in assay: 125 µM). The unlabeled peptide dilutions series was first prepared in 100% DMSO and then diluted 1:10 using the above-mentioned HEPES buffer system. Experiments were performed in triplicate and the data were fitted to a sigmoidal dose response curve (bottom constrain: 0) using GraphPad Prism (10.2.3).

6.3.2 Inhibition Assay

For the FP inhibition assay, 12 two-fold dilutions of un-labelled peptide were prepared in consistent buffer (same as for the protein tested). Then a probe-protein-mix was prepared by diluting 1xBSA, desired protein and working probe's stock in buffer to give double of in-assay concentrations (in-assay probe concentration: 50 nM TAMRA-labelled GluN2B peptide. Protein concentrations for the in-assay probe mix were calculated based on K_d of probe). The assay was then performed by adding 15 µL of peptide dilution and 15 µL of probe-protein-mix to each well. Blanks were prepared as described above (section 6.3.1). References were prepared by diluting the

working probe (probe-protein-mix) in buffer to in-assay concentrations and adding 30 µL to each well. The K_i values were calculated according to Nikolovska-Coleska et al. (2004).

6.4 Plasmin Stability Assay

Preheated (37ºC) PBS buffer (170 µL, 100 mM, pH 8.0) was spiked with peptide (20 µL) prepared as 500 µM stock in PBS buffer to reach a final concentration of 52.5 µM of peptide (<0.5% final DMSO). A time point “0 min” samples was collected by transferring 19 µL of assay matrix in 181 µL of MeCN/H 2 O (1:1). Next, the assay matrix was supplemented with reconstituted Plasmin (9 µL, concentration: 4 µg/µL; Plasmin from human plasma, ≥ 2.0 units/mg protein, Sigma Aldrich, CAS#: 9001-90-5) to reach a final concentration of 50 µM of peptide and 0.2 µg/µL Plasmin. Next, time point samples were collected at 0.5, 15, 30, 60 and 120 min by adding 20 µL of assay matrix to 180 µL of MeCN/H 2 O (1:1). The samples were vortexed, flash-frozen (15 min) and centrifuged at 13.400 rpm for 5 min- The supernatant was analyzed by LC-MS/MS in single-reaction monitoring (SRM) mode (precursor ion: m/z = 989.1, product ion: m/z = 245.9, collision energy = 42). The observed product ion intensity was integrated and the obtained area under the curve (AUC) for each time point and replicate was normalized (Microsoft Excel 2016) to the mean AUC of the entire PBS negative control (7 data points). The half-life (T 1/2) was determined by plotting (non-linear fit, one-phase decay; plateau = 0) the data in Graph Pad Prism (10.2.3). The data is represented as the mean of three individual experiments (n = 3).

7 References

Aarts, M. (2002). Treatment of Ischemic Brain Damage by Perturbing NMDA Receptor- PSD-95 Protein Interactions. *Science*, 298(5594), pp.846–850. doi:https://doi.org/10.1126/science.1072873.

Albericio, F., Bofill, J.M., El-Faham, A. and Kates, S.A. (1998). Use of Onium Salt-Based Coupling Reagents in Peptide Synthesis[1]. *The Journal of Organic Chemistry*, 63(26), pp.9678–9683. doi:https://doi.org/10.1021/jo980807y.

Alexopoulou, F. (2022). *PhD thesis, Flora Alexopoulou Targeting protein-protein interactions using peptide technologies*. Was provided digitally.

Andreasen, J.T., Bach, A., Gynther, M., Nasser, A., Mogensen, J., Strømgaard, K. and Pickering, D.S. (2013). UCCB01-125, a dimeric inhibitor of PSD-95, reduces inflammatory pain without disrupting cognitive or motor performance: Comparison with the NMDA receptor antagonist MK-801. *Neuropharmacology*, 67, pp.193–200. doi:https://doi.org/10.1016/j.neuropharm.2012.11.006.

Bach, A., Chi, C.N., Olsen, T.B., Pedersen, S.W., Røder, M.U., Pang, G.F., Clausen, R.P., Jemth, P. and Strømgaard, K. (2008). Modified Peptides as Potent Inhibitors of the Postsynaptic Density-95/*N*-Methyl-d-Aspartate Receptor Interaction. *Journal of Medicinal Chemistry*, 51(20), pp.6450–6459. doi:https://doi.org/10.1021/jm800836w.

Bach, A., Clausen, B.H., Møller, M., Vestergaard, B., Chi, C.N., Round, A., Sørensen, P.L., Nissen, K.B., Kastrup, J.S., Gajhede, M., Jemth, P., Kristensen, A.S., Lundström, P., Lambertsen, K.L. and Strømgaard, K. (2012). A high-affinity, dimeric inhibitor of PSD-95 bivalently interacts with PDZ1-2 and protects against ischemic brain damage. *Proceedings of the National Academy of Sciences*, 109(9), pp.3317–3322. doi:https://doi.org/10.1073/pnas.1113761109.

Balboa, J.R., Essig, D.J., Ma, S., Nichlas Karer, Clemmensen, L.S., Pedersen, S.W., Joerger, A.C., Knapp, S., Søren Østergaard and Strømgaard, K. (2022). Development of a Potent Cyclic Peptide Inhibitor of the nNOS/PSD-95 Interaction. *Journal of Medicinal Chemistry*, 66(1), pp.976–990. doi:https://doi.org/10.1021/acs.jmedchem.2c01803.

Bechtler, C. and Lamers, C. (2021). Macrocyclization strategies for cyclic peptides and peptidomimetics. *RSC Medicinal Chemistry*, [online] 12(8), pp.1325–1351. doi:https://doi.org/10.1039/D1MD00083G.

Behrendt, R., White, P. and Offer, J. (2016). Advances in Fmoc solid-phase peptide synthesis. *Journal of Peptide Science*, 22(1), pp.4–27. doi:https://doi.org/10.1002/psc.2836.

Blanke, M.L. and Antonius M.J. VanDongen (2009). *Activation Mechanisms of the NMDA Receptor*. [online] Nih.gov. Available at: https://www.ncbi.nlm.nih.gov/books/NBK5274/ [Accessed 5 Mar. 2024].

Chan, W. and White, P. (1999). *Fmoc Solid Phase Peptide Synthesis: A Practical Approach*. [online] *Google Books*. Oxford University Press. Available at: https://books.google.dk/books?hl=sv&lr=&id=wWR7DwAAQBAJ&oi=fnd&pg=PR9&ots=ohU7iCySoV&sig=tDXFrqb0Z4DxzbkQN8_DArslIV8&redir_esc=y#v=onepage&q&f=false [Accessed 8 Mar. 2024].

Choi, D.W. (1992). Excitotoxic Cell Death. *Journal of Neurobiology*, [online] 23(9), pp.1261–1276. doi:https://doi.org/10.1002/neu.480230915.

Christensen, N.R., Čalyševa, J., Fernandes, E.F.A., Lüchow, S., Clemmensen, L.S., Haugaard-Kedström, L.M. and Strømgaard, K. (2019). PDZ Domains as Drug Targets. *Advanced Therapeutics*, [online] 2(7). doi:https://doi.org/10.1002/adtp.201800143.

Cunningham, B. and Wells, J. (1989). High-resolution epitope mapping of hGH-receptor interactions by alanine-scanning mutagenesis. *Science*, 244(4908), pp.1081–1085. doi:https://doi.org/10.1126/science.2471267.

DeSai, C. and Hays Shapshak, A. (2023). *Cerebral Ischemia*. [online] PubMed. Available at: https://www.ncbi.nlm.nih.gov/books/NBK560510/ [Accessed 12 Feb. 2024].

El-Faham, A. and Albericio, F. (2011). Peptide Coupling Reagents, More than a Letter Soup. *Chemical Reviews*, 111(11), pp.6557–6602. doi:https://doi.org/10.1021/cr100048w.

Fields, G.B. (2001). Introduction to Peptide Synthesis. *Current Protocols in Protein Science*, [online] 26(1). doi:https://doi.org/10.1002/0471140864.ps1801s26.

Hill, M.D., Goyal, M., Menon, B.K., Nogueira, R.G., McTaggart, R.A., Demchuk, A.M., Poppe, A.Y., Buck, B.H., Field, T.S., Dowlatshahi, D., van Adel, B.A., Swartz, R.H., Shah, R.A., Sauvageau, E., Zerna, C., Ospel, J.M., Joshi, M., Almekhlafi, M.A., Ryckborst, K.J. and Lowerison, M.W. (2020). Efficacy and safety of nerinetide for the treatment of acute ischaemic stroke (ESCAPE-NA1): a multicentre, double-blind, randomised controlled trial. *The Lancet*, 395(10227). doi:https://doi.org/10.1016/s0140-6736(20)30258-0.

Hillier, B.J. (1999). Unexpected Modes of PDZ Domain Scaffolding Revealed by Structure of nNOS-Syntrophin Complex. *Science*, [online] 284(5415), pp.812–815. doi:https://doi.org/10.1126/science.284.5415.812.

Huang, X. (2003). Fluorescence Polarization Competition Assay: The Range of Resolvable Inhibitor Potency Is Limited by the Affinity of the Fluorescent Ligand. *SLAS Discovery*, 8(1), pp.34–38. doi:https://doi.org/10.1177/1087057102239666.

Iris Biotech (2021). *About the Advantages of Pseudoproline Dipeptides*. [online] Available at: https://www.iris-biotech.de/de/blog/about-the-advantages-of-pseudoproline-dipeptides/ [Accessed 14 Mar. 2024].

Ji, X., Nielsen, A.L. and Heinis, C. (2024). Cyclic Peptides for Drug Development. *Angewandte Chemie (International Ed. in English)*, [online] 63(3), p.e202308251. doi:https://doi.org/10.1002/anie.202308251.

Jilani, T.N. and Siddiqui, A.H. (2019). *Tissue Plasminogen Activator*. [online] National Library of Medicine. Available at: https://www.ncbi.nlm.nih.gov/books/NBK507917/.

Joo, S.H. (2012). Cyclic Peptides as Therapeutic Agents and Biochemical Tools. *Biomolecules & Therapeutics*, [online] 20(1), pp.19–26. doi:https://doi.org/10.4062/biomolther.2012.20.1.019.

Kaiser, E., Colescott, R.L., Bossinger, C.D. and Cook, P.I. (1970). Color test for detection of free terminal amino groups in the solid-phase synthesis of peptides. *Analytical Biochemistry*, 34(2), pp.595–598. doi:https://doi.org/10.1016/0003-2697(70)90146-6.

Kempson, J., Zhao, R., Pawluczyk, J., Wang, B., Zhang, H., Hou, X., Allen, M.P., Wu, D.-R., Li, P., Yip, S., Smith, A., Traeger, S.C., Huang, S., Cutrone, J., Mukherjee, S., Sfouggatakis, C., Poss, M., Scola, P.M., Meanwell, N.A. and Carter, P.H. (2024). Challenges with the Synthesis of a Macrocyclic Thioether Peptide: From Milligram to Multigram Using Solid Phase Peptide Synthesis (SPPS). *Journal of organic chemistry*. doi:https://doi.org/10.1021/acs.joc.4c00429.

Lee, H.-J. and Zheng, J.J. (2010). PDZ domains and their binding partners: structure, specificity, and modification. *Cell Communication and Signaling*, 8(1). doi:https://doi.org/10.1186/1478-811x-8-8.

Lukszo, J., Patterson, D., Albericio, F. and Kates, S.A. (1996). 3-(1-Piperidinyl)alanine formation during the preparation ofC-terminal cysteine peptides with the Fmoc/t-Bu strategy. *Letters in peptide science*, 3(3), pp.157–166. doi:https://doi.org/10.1007/bf00132978.

Marder, O., Youval Shvo and Albericio, F. (2003). HCTU and TCTU: New Coupling Reagents — Development and Industrial Aspects. *Chem Inform*, 34(32). doi:https://doi.org/10.1002/chin.200332258.

Mayor-Nunez, D., Ji, Z., Sun, X., Teves, L., Garman, J. and Tymianski, M. (2021). Plasmin-resistant PSD-95 inhibitors resolve effect-modifying drug-drug interactions between alteplase

and nerinetide in acute stroke. *Science Translational Medicine*, 13(588). doi:https://doi.org/10.1126/scitranslmed.abb1498.

Moerke, N.J. (2009). Fluorescence Polarization (FP) Assays for Monitoring Peptide-Protein or Nucleic Acid-Protein Binding. *Current Protocols in Chemical Biology*, 1(1), pp.1–15. doi:https://doi.org/10.1002/9780470559277.ch090102.

Mthembu, S.N., Chakraborty, A., Schönleber, R., Albericio, F. and de la Torre, B.G. (2022). Solid-Phase Synthesis of C-Terminus Cysteine Peptide Acids. *Organic Process Research & Development*, 26(12), pp.3323–3335. doi:https://doi.org/10.1021/acs.oprd.2c00321.

Nikolovska-Coleska, Z., Wang, R., Fang, X., Pan, H., Tomita, Y., Li, P., Roller, P.P., Krajewski, K., Saito, N.G., Stuckey, J.A. and Wang, S. (2004). Development and optimization of a binding assay for the XIAP BIR3 domain using fluorescence polarization. *Analytical Biochemistry*, [online] 332(2), pp.261–273. doi:https://doi.org/10.1016/j.ab.2004.05.055.

Olsen, J.V., Ong, S.-E. and Mann, M. (2004). Trypsin cleaves exclusively C-terminal to arginine and lysine residues. *Molecular & cellular proteomics : MCP*, [online] 3(6), pp.608–14. doi:https://doi.org/10.1074/mcp.T400003-MCP200.

Prystay, L., Gosselin, M. and Banks, P. (2001). Determination of Equilibrium Dissociation Constants in Fluorescence Polarization. *SLAS Discovery*, 6(3), pp.141–150. doi:https://doi.org/10.1177/108705710100600304.

RCSB Protein Data Bank (2012). *RCSB PDB - 3ZRT: Crystal structure of human PSD-95 PDZ1-2*. [online] www.rcsb.org. Available at: https://www.rcsb.org/structure/3ZRT [Accessed 27 May 2024].

Serrano, M.E., Kim, E., Petrinovic, M.M., Turkheimer, F. and Cash, D. (2022). Imaging Synaptic Density: The Next Holy Grail of Neuroscience? *Frontiers in Neuroscience*, 16. doi:https://doi.org/10.3389/fnins.2022.796129.

SubirÃ³s-Funosas, R., Prohens, R., Barbas, R., El-Faham, A. and Albericio, F. (2009). Oxyma: An Efficient Additive for Peptide Synthesis to Replace the Benzotriazole-Based HOBt and HOAt with a Lower Risk of Explosion[1]. *Chemistry - A European Journal*, 15(37), pp.9394–9403. doi:https://doi.org/10.1002/chem.200900614.

Tanada, M., Minoru Tamiya, Matsuo, A., Aya Chiyoda, Takano, K., Ito, T., Irie, M., Kotake, T., Takeyama, R., Kawada, H., Hayashi, R., Ishikawa, S., Nomura, K., Noriyuki Furuichi, Morita, Y., Kage, M., Hashimoto, S., Nii, K., Hitoshi Sase and Ohara, K. (2023). Development of Orally Bioavailable Peptides Targeting an Intracellular Protein: From a Hit to a Clinical KRAS Inhibitor. *Journal of the American Chemical Society*, 145(30), pp.16610–16620. doi:https://doi.org/10.1021/jacs.3c03886.

Torsten Wöhr, Wahl, F., Adel Nefzi, Rohwedder, B., Sato, T., Sun, X. and Mutter, M. (1996). Pseudo-Prolines as a Solubilizing, Structure-Disrupting Protection Technique in Peptide Synthesis. *Journal of the American Chemical Society*, 118(39), pp.9218–9227. doi:https://doi.org/10.1021/ja961509q.

Ugalde-Triviño, L. and Díaz-Guerra, M. (2021). PSD-95: An Effective Target for Stroke Therapy Using Neuroprotective Peptides. *International Journal of Molecular Sciences*, [online] 22(22), p.12585. doi:https://doi.org/10.3390/ijms222212585.

Wu, M.-C. and Tian Yow Tsong (2013). Local Hydrophobicity in Protein Secondary Structure Formation. *Journal of the Physical Society of Japan*, 82(11), pp.114801–114801. doi:https://doi.org/10.7566/jpsj.82.114801.

Zhang, J., Lewis, Steven M., Kuhlman, B. and Lee, Andrew L. (2013). Supertertiary Structure of the MAGUK Core from PSD-95. *Structure*, 21(3), pp.402–413. doi:https://doi.org/10.1016/j.str.2012.12.014.

Appendix A

Successfully synthesized peptides including UPLC chromatograms and Mass spectra

Table A1: Exp. = expected m/z value (calculated); obs. = observed m/z value.

Peptide	Sequence	Mass	$[M+H]^+$		$[M+2H]2^+$		$[M+H+Na]^{2+}$	
			exp.	obs.	exp.	obs.	exp.	obs.
1	*Cyclic*[fIETTFAGNRIETSFTC]	1974.91	1975.9	1977.2	988.5	988.5	999.5	999.7
11	*Cyclic*[fIETTFAGNRIETSF**A**C]	1944.90	1945.9	1946.8	973.5	973.5	984.5	984.5
12	*Cyclic*[fIETTFAGNRIETS**A**TC]	1898.88	1899.9	1901.1	950.4	950.8	961.4	961.5
13	*Cyclic*[fIETTFAGNRIET**A**FTC]	1958.92	1959.9	1960.6	980.5	981.6	991.5	991.5
14	*Cyclic*[fIETTFAGNRIE**A**SFTC]	1944.90	1945.9	1946.7	973.5	973.5	984.5	984.6
15	*Cyclic*[fIETTFAGNRI**A**TSFTC]	1916.19	1917.2	1919.6	959.1	959.1	970.1	971.1
16	*Cyclic*[fIETTFAGNR**A**ETSFTC]	1932.87	1933.9	1934.8	967.4	967.4	978.4	978.7
21	*Cyclic*[fIET**A**FAGNRIETSFTC]	1944.90	1945.9	1946.9	973.5	973.6	984.5	984.5
23	*Cyclic*[fI**A**TTFAGNRIETSFTC]	1916.91	1917.2	1918.2	959.1	959.5	970.1	970.1
24	*Cyclic*[f**A**ETTFAGNRIETSFTC]	1932.87	1933.9	1934.8	967.4	967.4	978.4	978.6

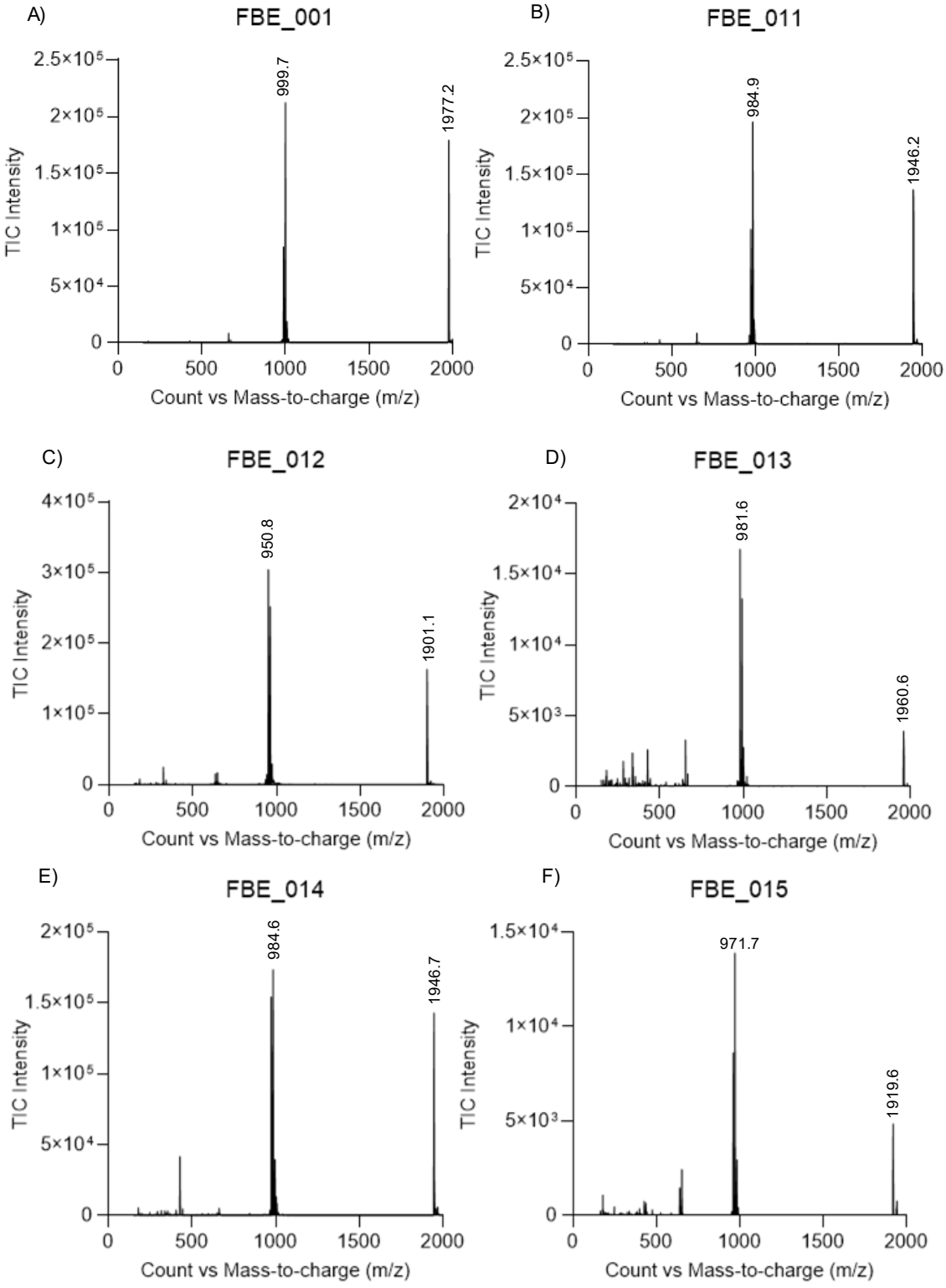
A)
FBE_001
999.7
1977.2
TIC Intensity
Count vs Mass-to-charge (m/z)
B)
FBE_011
984.9
1946.2
TIC Intensity
Count vs Mass-to-charge (m/z)
C)
FBE_012
950.8
1901.1
TIC Intensity
Count vs Mass-to-charge (m/z)
D)
FBE_013
981.6
1960.6
TIC Intensity
Count vs Mass-to-charge (m/z)
E)
FBE_014
984.6
1946.7
TIC Intensity
Count vs Mass-to-charge (m/z)
F)
FBE_015
971.7
1919.6
TIC Intensity
Count vs Mass-to-charge (m/z)

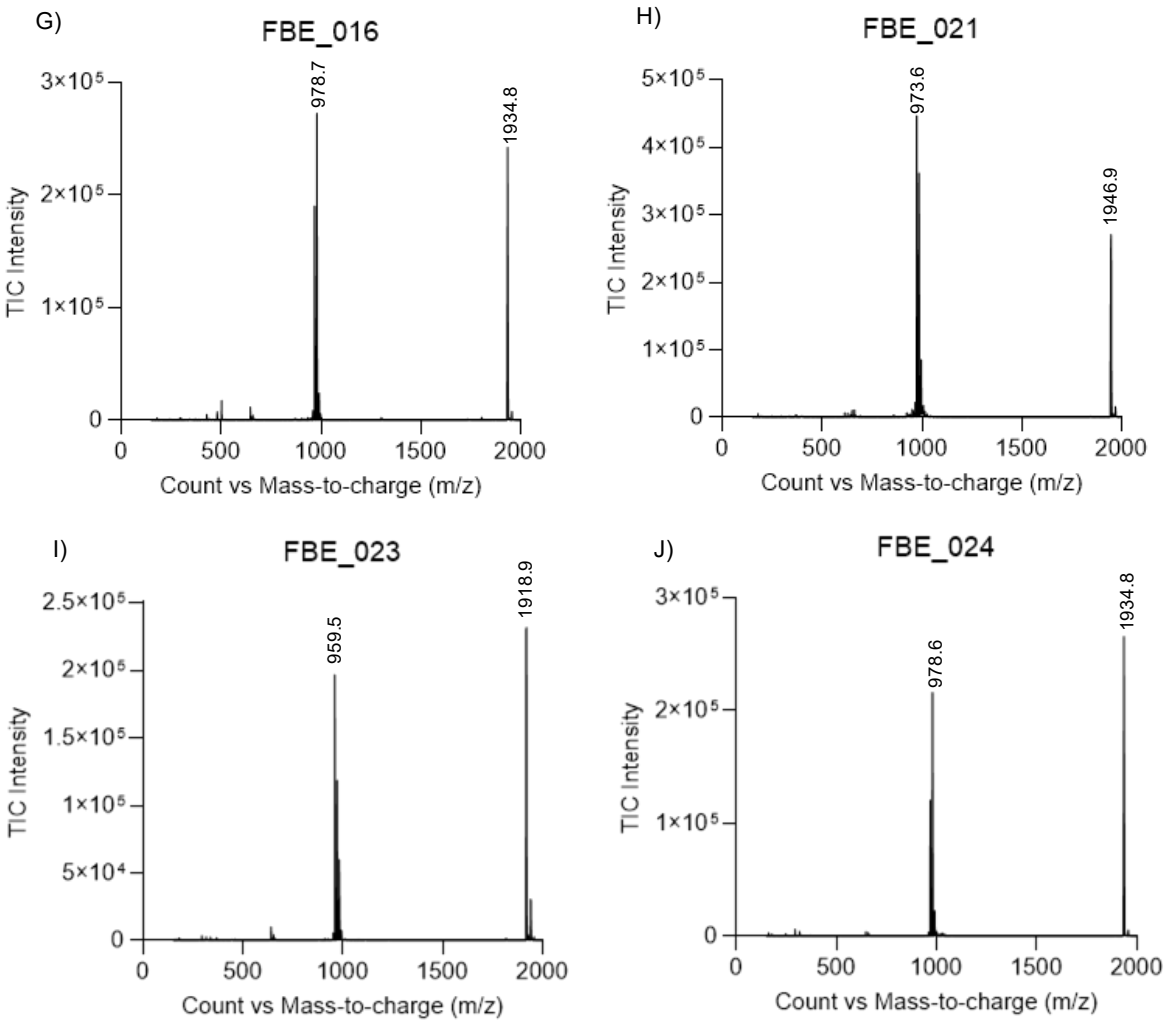

Figure A1: LC-MS spectra of peptides FBE_01-024. A) LC-MS of FBE_001. B) LC-MS of FBE_011. C) LC-MS of FBE_012. D) LC-MS of FBE_013. E) LC-MS of FBE_014. F) LC-MS of FBE_015. G) LC-MS of FBE_016. H) LC-MS of FBE_021. I) LC-MS of FBE_023. J) LC-MS of FBE_024.

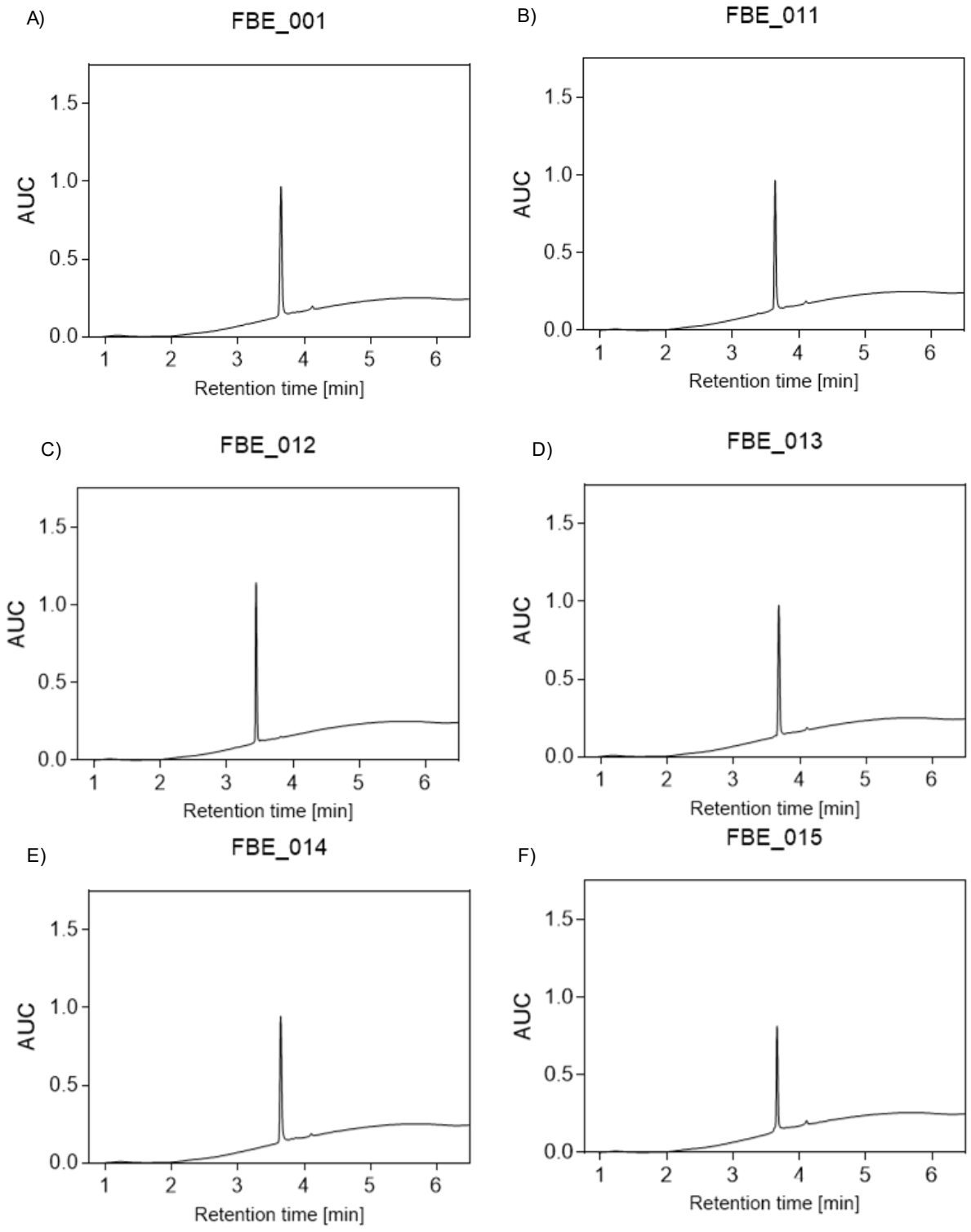
A)
FBE_001
AUC
Retention time [min]
B)
FBE_011
AUC
Retention time [min]
C)
FBE_012
AUC
Retention time [min]
D)
FBE_013
AUC
Retention time [min]
E)
FBE_014
AUC
Retention time [min]
F)
FBE_015
AUC
Retention time [min]

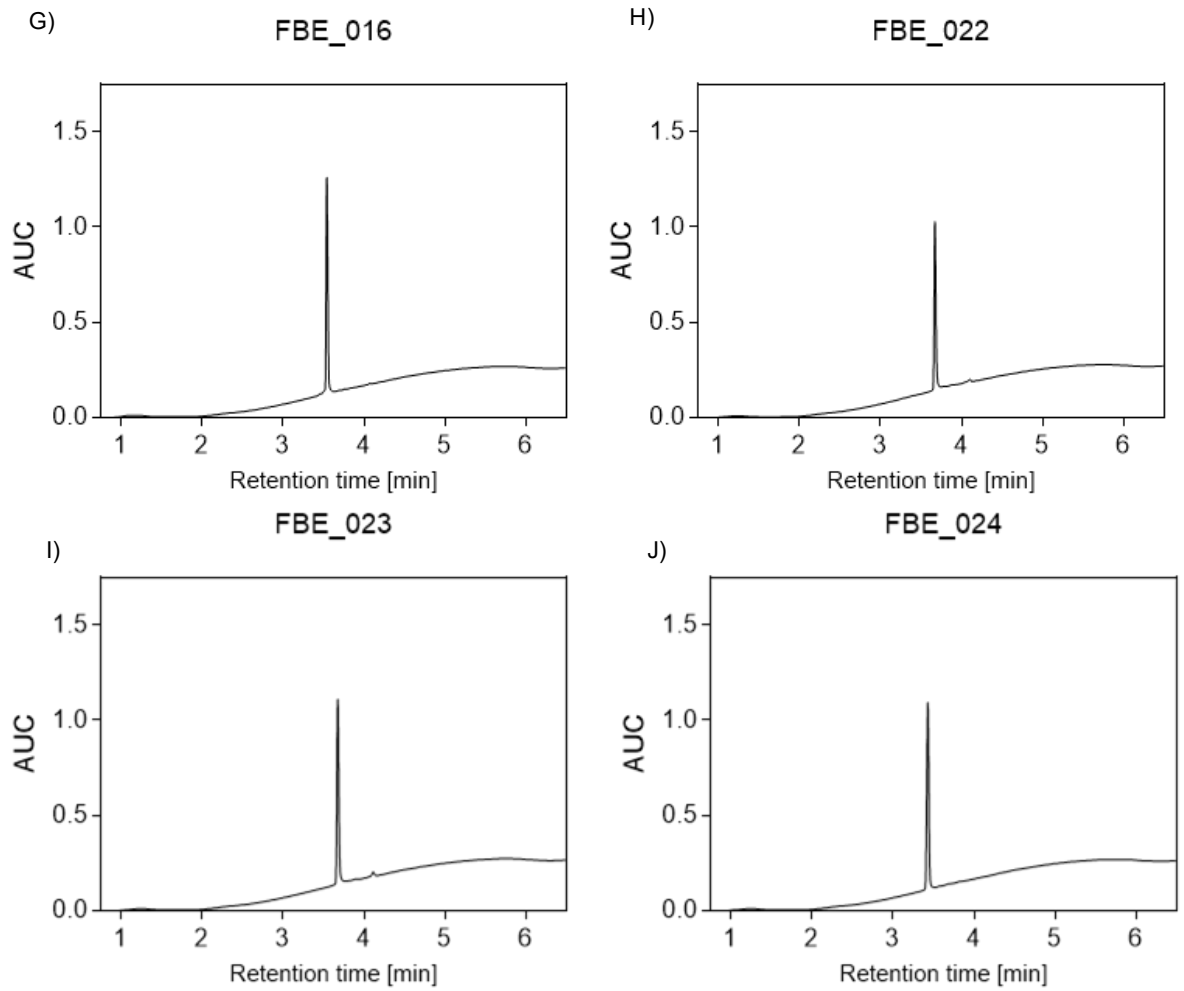

Figure A2: UPLC chromatograms of peptides FBE_01-024. A) UPLC of FBE_001. B) UPLC of FBE_011. C) UPLC of FBE_012. D) UPLC of FBE_013. E) UPLC of FBE_014. F) UPLC of FBE_015. G) UPLC of FBE_016. H) UPLC of FBE_021. I) UPLC of FBE_023. J) UPLC of FBE_024.